Marquette University
e-Publications@Marquette

Dissertations (2009 -) | Dissertations, Theses, and Professional Projects

Neuromodulation for Depression: Insights Gained from Neuroimaging and Computational Models

Yagna Pathak
Marquette University

Recommended Citation
Pathak, Yagna, "Neuromodulation for Depression: Insights Gained from Neuroimaging and Computational Models" (2014). *Dissertations (2009 -)*. Paper 418.
http://epublications.marquette.edu/dissertations_mu/418

NEUROMODULATION FOR DEPRESSION: INSIGHTS GAINED FROM NEUROIMAGING AND COMPUTATIONAL MODELS

By

Yagna Pathak, B.S., M.Eng

A Dissertation submitted to the Faculty of the Graduate School,
Marquette University,
in Partial Fulfillment of the Requirements for
the Degree of Doctor of Philosophy

Milwaukee, Wisconsin

December 2014

ABSTRACT
NEUROMODULATION FOR DEPRESSION: INSIGHTS GAINED FROM NEUROIMAGING AND COMPUTATIONAL MODELS

Yagna Pathak, B.S., M.Eng.

Marquette University, 2014

Major depressive disorder (MDD) is a public health concern worldwide, affecting a sixth of the American population. Neuromodulation therapies have been employed to treat severe cases of treatment resistant depression. These procedures attempt to modulate activity in cortical regions that represent nodes in brain circuits believed to be involved in MDD. One challenge in neuromodulation trials has been the difficulty in quantifying outcome variability. We sought to understand the effects of neuromodulation therapies and their sources of variability while adding an objective perspective to assess clinical improvement in neuropsychiatric disorders such as depression.

The goal of my dissertation was to investigate the neuronal circuitry of MDD patients who were treated using neuromodulation. Our primary measures were behavior scores and results from functional neuroimaging. The specific aims of this study were to answer three fundamental questions: 1) What is the role of stimulation parameters in patient response to chronic epidural cortical stimulation (EpCS) for MDD? 2) What functional changes result from repetitive transcranial magnetic stimulation (rTMS) for MDD? 3) How does stimulation of different targets in the depressive circuit affect antidepressive response? Our results suggest that combining neuroimaging with computational tools can increase the predictive power to determine who is likely to respond to a specific neuromodulation treatment course. We demonstrated the significance of stimulation parameters (location, polarity, duration) and the engagement of crucial nodes of the depressive circuit in order to achieve a sustained clinical improvement. Additionally, we showed that it is possible to affect deeper brain regions by targeting superficial areas that are easier to access with noninvasive modalities. The approaches highlighted in this dissertation can provide valuable insights about patients evaluated for neuromodulation for depression.

ACKNOWLEDGEMENTS

Yagna Pathak, B.S., M.Eng.

I am beyond grateful for the amazing mentorship of Dr. Chris Butson, my adviser through this process. His guidance has enabled me to think progressively and approach research with a bold attitude. His constant encouragement and honest advice has been instrumental in my success. Next, I would like to thank members of my lab, Brian Goodwin, Klaus Driesslein, Dr. Xuefeng. Wei, and Sanket Jain. Whether it was to brainstorm a new concept or merely rant, these folks have been there with invaluable words of wisdom. I would also like to express my gratitude towards my dissertation committee members, Dr. Dami Salami, Dr. Joe Goveas, Dr. Scott Beardsley, and Dr. Taly Gilat-Schmidt, whose expertise was constructive to my project and helped it evolve.

Additionally, I would like to thank Dr. Sylvain Baillet at McGill University, who organized an incredibly productive week in Montreal for me to learn MEG processing and continually offered his invaluable insight on the TMS portion of my project. I would also like to acknowledge Dr. Clement Hamani at the University of Toronto for providing the data for my DBS aim and offering a surgical perspective that made this project more translational and therefore, relevant.

Furthermore, I want to recognize the efforts of Mary Wesley, Dr. Lars Olson and Dr. Kris Ropella in the Department of Biomedical Engineering. It is their support and advice that enabled me to travel for conferences, submit paperwork on time and choose appropriate courses. Also, I would like to acknowledge the Medical College of

Wisconsin, specifically, Center for Imaging Research, Biotechnology & Bioengineering Center, and the Departments of Neurology, Neurosurgery and Psychiatry. They provided me with resources and guidance necessary to implement the work presented here.

The most special thanks to my family: my mother, Ranjana Pathak, who loves me unconditionally and expressed that through numerous home-made meals she brought to me over the last four years, my father, Jyotish Pathak, who instilled in me a passion for engineering at a very young age and continues to inspire me every day, and my sister, Neha Pathak, who patiently shared every moment of this journey with me as my roommate and best friend. She smiled enthusiastically during various mock presentations, celebrated my every little success and comforted me during stressful times. I would also like to acknowledge my school teachers and my mentors at Illinois Institute of Technology and Cornell University who shaped my curiosity and led me to this path. Finally, I want to thank my friends, especially the ones in Milwaukee, for their relentless support, intelligent discussions and constant inspiration.

TABLE OF CONTENTS

GLOSSARY

AP	action potential
BDNF	brain-derived neurotrophic factor
CSF	cerebrospinal fluid
CT	computed tomography
Coherence	magnitude squared coherence
DBS	deep brain stimulation
DTI	diffusion tensor imaging
ECT	electroconvulsive therapy
EEG	electroencephalography
EKG	electrocardiography
EOG	electrooculography
EpCS	chronic epidural cortical stimulation
fMRI	functional magnetic resonance imaging
HDRS	Hamilton depression rating scale
IPG	implantable pulse generator
L-DLPFC	left dorsolateral prefrontal cortex
MADRS	Montgomery-Asberg depression rating scale
MDD	major depressive disorder
MEG	magnetoencephalography
MRI	magnetic resonance imaging
NAc	nucleus accumbens

OFC	orbitofrontal cortex
pACC	pregenual anterior cingulate cortex
PAG	periaqueductal gray area
PET	positron emission tomography
PFC	prefrontal cortex
Pial surface	outermost layer of the cerebral cortex
PSD	power spectral density
ROI	region of interest
RMT	resting motor threshold
rTMS	repetitive transcranial magnetic stimulation
sACC	subgenual anterior cingulate cortex
VMPFC	ventromedial prefrontal cortex
VNS	vagal nerve stimulation
VT area	ventral tegmental area
VTA	volume of tissue activation
WMF	white matter fibers
wMNE	weighted Minimum-Norm Estimate

SPECIFIC AIMS

Nearly one-sixth of the American population is affected by depression over the course of their lifetime. Major depressive disorder MDD occurrence has increased, making it a leading cause of disability worldwide. Previous studies have focused on empirical observations of therapeutic effects without a detailed explanation of clinical improvement. Due to variable efficacy of pharmacological treatments, neuromodulation has emerged as a lucrative option. The goal of my doctoral work was to examine the neuronal circuitry involved in MDD by combining neuroimaging and computational tools. Through the studies outlined below, we established the ability of these translational techniques to increase the predictive power of a robust clinical response. The results and methods contribute to current knowledge by guiding the evaluation of patients treated with neuromodulation for depression.

Specific Aim 1: What is the role of stimulation parameters in patient response to EpCS for MDD?

Our hypothesis was that the degree of variability in patient response to EpCS can be attributed to the parameters of the stimulation protocol. Our results demonstrated that stimulation polarity, electrode location, and duration of stimulation are important factors in determining the effectiveness of this therapy.

Specific Aim 2: What functional changes result from rTMS for MDD?

In this study, we hypothesized that modulation of L-DLPFC can be assessed with resting-state functional imaging. We demonstrated changes in PSD and functional connectivity between important regions of the MDD circuit. Lastly, we also showed that

noninvasive approaches can be used to interrogate deeper brain areas and, consequently, guide future DBS studies.

Specific Aim 3: How does stimulation of different targets in the depressive circuit affect antidepressive response?

This aim was motivated by previous reports of variable outcomes of DBS for depression. Our hypothesis for this aim was that improvement in depressive behavior would be dependent on stimulation within the MDD circuit and at a particular target. Our results confirmed the differential involvement of different nodes in MDD pathology while emphasizing the need to continue our investigation in this field with the perspective of circuit-based therapeutic options for MDD.

CHAPTER 1: BACKGROUND/SIGNIFICANCE

I. Major Depressive Disorder

A. General Impact and Neurobiology

MDD affects approximately 14 million Americans every year (Lisanby, 2007). According to the World Health Organization, it will be the second most common cause of disability by the year 2020. It impairs the patient's quality of life and can lead to death by suicide. It is characterized by depressed mood, anhedonia, irritability, poor concentration, feelings of hopelessness, thoughts of self-harm, inappropriate guilt, and abnormal appetite and sleep patterns (Kopell et al., 2011; Krishnan & Nestler, 2008; Mayberg, 1997). The rate of response to antidepressant medications is as low as 50%. According to the STAR*D trial (Rush et al., 2006), the remission rate decreases as treatment steps (number of medications) increase. Because of its significant impact on the general population and lost productivity, it is important to better understand the causes and underlying mechanisms of MDD.

MDD is clinically heterogeneous. The diagnosis and assessment for improvement are also subjective (Krishnan & Nestler, 2008). No clinically suitable methods have been developed to predict treatment response (Ramasubbu & MacQueen, 2010). In addition, several models have been proposed, but with limited data to validate those findings or use them for effective therapy options.

MDD is a circuit-based disorder with several regions of the brain (prefrontal cortex (PFC), amygdala, striatum, pallidum, and medial thalamus) functionally aberrant (Drevets et al., 1992). Activity in the limbic regions, specifically the amygdala and

anterior cingulate cortex (ACC) (Brodmann's area 25), is associated with depressive symptoms. Several hypotheses have been proposed to characterize MDD. The monoamine hypothesis (Krishnan & Nestler, 2008; Pittenger & Duman, 2008) suggests that a decrease in monoamine function can lead to depression. Among the monoamine projections from mid-brain to brainstem nuclei are 1) dopamine from the ventral tegmental area (VT area), 2) serotonin from dorsal raphe in the periaqueductal gray area (PAG), and 3) noradrenaline from locus coerulus. Secondary neuroplasticity on a cellular level is also induced by some antidepressants that acutely increase synaptic monoamines. In addition, the brain-derived neurotrophic factor (BDNF) hypothesis (Krishnan & Nestler, 2008; Nestler & Carlezon, 2006; Pittenger & Duman, 2008) implies that an increase in BDNF at the VT area and nucleus accumbens (NAc) may increase neurovegetative symptoms associated with depression.

B. Key Regions

Abnormalities in the cortico-limbic structure and function are commonly identified in MDD (Mayberg, 2003; Ramasubbu & MacQueen, 2010). For noninvasive and minimally invasive methods of neuromodulation, the immediate target must be superficial for easy access. The left dorsolateral prefrontal cortex (L-DLPFC), which is hypometabolic (Koenigs & Grafman, 2009; Mayberg, 2003) in MDD, tends to be an effective target for rTMS and EpCS. For more invasive techniques such as DBS, the subgenual anterior cingulate cortex (Hamani et al., 2009; Ressler & Mayberg, 2007) (sACC), amygdala, and NAc (Bewernick et al., 2010, 2012) are common targets and tend to be hypermetabolic (Figure 1).

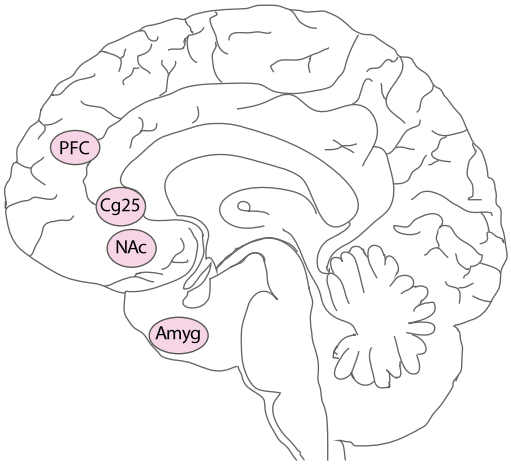

Figure 1.1: Key regions that are affected in the depressive circuit (Adapted from Krishnan 2008)

L-DLPFC: The role of L-DLPFC in neuropsychological disorders has been investigated extensively. DLPFC is implicated in cognitive and executive function, receives input from specific sensory cortices, and has interconnections with premotor areas, frontal eye fields, and the lateral parietal cortex (Koenigs & Grafman, 2009). Morphological changes associated with depression include decreased cortical thickness, decreased neuronal and glial densities, and decreased neuronal size (Miller & Cummings, 2007; Rajkowska et al., 1999). The role of the PFC in depression is demonstrated in the literature through imaging and lesion studies. A region-of-interest (ROI) analysis revealed that connectivity between the dorsal cingulate cortex and three other regions (medial thalamus, amygdala, and pallidostriatum) was reduced in depressed patients when compared with controls (Anand et al., 2005a; Ramasubbu & MacQueen, 2010). One recent resting-state functional magnetic resonance imaging (fMRI) study (Fox, Buckner, et al., 2012) showed that better clinical efficacy was found when L-DLPFC coordinates were negatively correlated with the sACC. This study further suggests that

part of the antidepressant mechanism of noninvasive neuromodulation involves altering activity at distal nodes such as the sACC, which plays a significant role in MDD.

sACC: The relevance of sACC in depression has been reported consistently. Anatomically, a decrease in glial density at this region has been associated with depression (Cotter et al., 2001; Miller & Cummings, 2007; Ongur et al., 1998). Activity in sACC couples with activity in the medial thalamus, thereby contributing to limbic-cortical dysregulation (Greicius et al., 2007; Mayberg, 1997). In one study, the length of a depressive episode correlated positively with functional connectivity in sACC (Greicius et al., 2007). The sACC is implicated in emotional and affective functions; it has projections to ventral striatum to modulate the reward and motivation circuit (Johansen-Berg et al., 2008; Koenigs & Grafman, 2009) and to PAG, hypothalamus, NAc, and amygdala to regulate visceral activity associated with emotion (Banks et al., 2007; Koenigs & Grafman, 2009).

Amygdala: Amygdala plays a major role in emotional regulation and memory formation (Canli et al., 2000; Drevets, 2001; Le Doux, 1996; Phelps et al., 1997). This region is typically hypermetabolic in depression. Increased blood flow at the amygdala has been observed in depression and during presentation of negative stimuli (Drevets, 2001; Drevets et al., 1992). Additionally, electrical stimulation of this area can evoke emotional memories (Brothers et al., 1990; Gloor et al., 1982). Structural asymmetry of this region has been documented for psychiatric conditions (Lu et al., 2013; Monkul et al., 2007; Morris et al., 1998). Norepinephrine released at the amygdala is a critical player in emotional learning and is elevated in depressed individuals (Drevets, 2001; Veith et al., 1994) Previous studies have also demonstrated coupling between amygdala

and both the DLPFC and sACC during negative affect (Banks et al., 2007; Drevets, 2001). The PFC has an inhibitory effect at this site in a top-down manner (Quirk & Beer, 2006). Fibers projecting from the PFC terminate on the inhibitory interneurons of the amygdala (Carmichael & Price, 1995; McDonald et al., 1996). Furthermore, the amygdala shares reciprocal anatomical connections with the ACC, orbitofrontal cortex (OFC), and dorsal medial prefrontal cortex (DMPFC) (Amaral & Price, 1984; Banks et al., 2007; Ghashghaei et al., 2007). Lastly, a recent MEG study showed an increased connectivity between the ACC and left amygdala in high frequency bands (Lu et al., 2013).

NAc: Anhedonia is a major symptom of severe depression and, therefore, NAc, which is a critical component of the reward circuit and a motivational link between the limbic and motor regions, has been investigated as a potential target for neuromodulation therapy (Krishnan & Nestler, 2008; Schlaepfer et al., 2008). Neuroimaging studies show increases in neuron activity at the NAc and increases in dopamine release in response to euphoric experiences. In the context of limbic regulation, a recent animal study demonstrated a dysfunctional reward system in mice exposed to social defeat stress that was then reversed by administering antidepressants (Berton et al., 2006; Schlaepfer et al., 2008). Anatomically, NAc has reciprocal connections with amygdala and the medial PFC. In addition, it receives projections from dopaminergic regions such as the VT area, OFC, and motor areas (dorsal caudate and globus pallidus). It also indirectly projects to the sACC, ventral pallidum, thalamus, and hypothalamus (Jones & Mogenson, 1980; Kelley & Stinus, 1984; Mogenson et al., 1983; Nauta & Domesick, 1984). Several of these regions are also implicated in depression. In a preliminary study investigating DBS

at this target, clinical improvement was observed following stimulation, which was further reflected through metabolic changes at specific sites measured with PET (Schlaepfer et al., 2008).

II. Neuromodulation for Depression

The current gold standard in neuromodulation treatment for MDD is electroconvulsive therapy (ECT) (Carpenter et al., 2009). However, sustained response is difficult and ECT efficacy varies with remission rates reported within the range of 20-80% (Carpenter et al., 2009; Sackeim, 2001). Also, this therapy is accompanied by an array of side effects including anterograde and retrograde amnesia, headaches, muscle aches, nausea, and fatigue (Carpenter et al., 2009; Fujita et al., 2006; Moscrip et al., 2006). As a result, there is a need for safer and more reliable interventions. Thus, neuromodulation techniques such as vagal nerve stimulation (VNS), chronic epidural stimulation (EpCS), repetitive transcranial magnetic stimulation (rTMS), and deep brain stimulation (DBS) are being investigated as treatment options.

A. Chronic Epidural Cortical Stimulation (EpCS)

EpCS is a minimally invasive method of cortical stimulation in which electrodes are implanted between the dura mater and the skull over the ROI for therapeutic benefits. Effects of EpCS depend on stimulation parameters such as electrode location, frequency, amplitude, pulse width, duty cycle, and polarity (Lefaucheur, 2008; Ranck, 1975). This method of stimulation targets pyramidal neurons located in the superficial layers of the cortex (Manola et al., 2005, 2007). Because each stimulation parameter has a specific effect, a combination of settings can be employed to initiate a cascade that will affect

both proximal and distal neural elements. Stimulation location and polarity are influential variables in achieving a specific circuit-level result. For example, a cathode preferentially hyperpolarizes neurons parallel to the electrode surface whereas an anode depolarizes neurons perpendicular to it (Lefaucheur, 2008; McIntyre & Grill, 1999).

B. Repetitive Transcranial Magnetic Stimulation (rTMS)

TMS is a noninvasive neurostimulation method to modulate the brain. The first TMS device to stimulate the cortex was designed by Barker and Cain in 1985 (Barker et al., 1985). Since then, the device has evolved with a plethora of stimulation parameters and coil geometries to target a specific region of the brain. It works through the principle of induction as described by Faraday. A magnetic field, generated by the current in the TMS coil, induces an electrical field in the underlying cerebral cortex, which causes local depolarization of pyramidal neurons (Figure 2) (Carpenter et al., 2009; Cohen et al., 1991; Ridding & Rothwell, 2007; Roth et al., 1991). This method can be viewed as introducing noise into the neural system. It is an attractive method because of its potential for high spatial and temporal resolution (Walsh & Cowey, 2000). However, the field declines logarithmically with optimal depth of depolarization at 2 cm with the figure-8 coil (George et al., 1999). Therefore, superficial structures make better targets for TMS therapy.

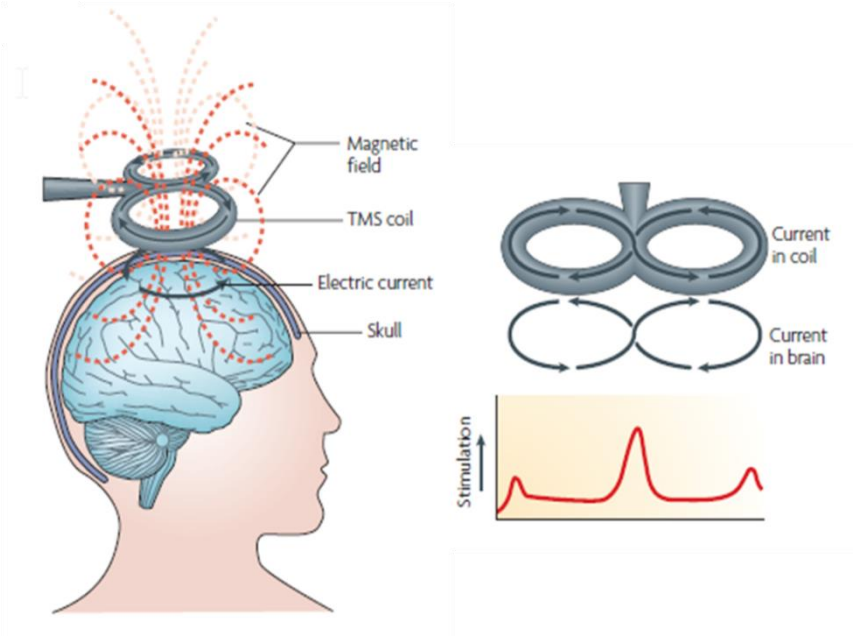

Figure 1.2: Physics of TMS. This figure was reprinted with permission from Ridding et al. Nature Reviews Neuroscience (2007)

Neuronal activity can be altered directly beneath the coil and at distant areas by mediating functional connections of these networks (Walsh & Cowey, 2000). A series of pulses is referred to as a train and application of these trains is defined as repetitive TMS (rTMS). Studies have investigated rTMS as both a priming method and a treatment option for depression (Fitzgerald et al., 2008, 2009). Location of stimulation and intensity are important parameters in rTMS therapy. Slow rTMS (< 1 Hz) has shown to be inhibitory whereas fast rTMS (> 5 Hz) is excitatory (Burt et al., 2002; Chen et al., 1997; Lefaucheur, 2008; Nakamura et al., 1997). Typically, the field strength is around 1.5 T for biphasic pulses and stimulation is applied at 10 Hz with a 5-second 'ON' period (Demitrack, 2007; Fitzgerald et al., 2009; O'Reardon et al., 2007) at the L-DLPFC (Nahas et al., 2001; Pascual-Leone et al., 1999). The intensity of stimulation depends on the individual's resting motor threshold (RMT), which can be measured by stimulation at

the hand-knob region of the motor cortex. Efficacy has been reported with rTMS applied in the range of 80-120% of RMT. The specific mechanisms of action are still unclear; however, an increase in BDNF has been reported poststimulation in both animal and human studies (Muller et al., 2000; Shimizu et al., 2003).

C. Deep Brain Stimulation (DBS)

DBS has been instrumental in shaping the field of neuromodulation for psychiatry and adding to our understanding of neurological disorders. The success of DBS for movement disorders, specifically Parkinson's disease, is a milestone in the field of functional neurosurgery. Many of these success stories have also reported improvement in affective symptoms, which has led to an extensive investigation of appropriate targets for neuropsychiatric disorders. DBS is the most invasive of the methods we focused on in this dissertation. It combines medical imaging (MRI + CT), neuronavigation, and physiological mapping to ensure correct placement of the electrode within the brain. During the procedure, the patient is awake but sedated (Greenberg, 2009). For specific disorders, appropriate targets have been explored based on results of lesion studies and advances in functional neuroimaging. The sACC and NAc of the striatum have been popular candidates for DBS for depression (Hamani et al., 2009; Malone et al., 2009; Mayberg et al., 2005; Riva-Posse et al., 2014).

The specific mechanisms of action for DBS remain open for debate. Many studies report contradictory effects, suggesting a combination of inhibitory and excitatory mechanisms to recruit cell bodies and axons depending mostly on the orientation of neural elements relative to electrode location. Other hypotheses have hinted at an inhibitory effect of high frequency DBS by activating GABAergic terminals or blocking

voltage-gated ion channels (Benabid et al., 2005; Greenberg, 2009). Simplistically, DBS has also been described as a functional lesion that modifies neurotransmission by implicating synaptic fatigue (Benabid et al., 2005; Rauch et al., 2006).

CHAPTER 2: GENERALIZED EXPERIMENTAL METHODS

I. Neuroimaging

Cognitive processing is an underlying function of networks that connect the major brain regions, and neuroimaging can be combined with neuromodulation to further extract information about local responses and remote interactions (Siebner et al., 2009; Thut & Pascual-Leone, 2010). Multimodal imaging offers improved prediction of outcomes and a better understanding of the brain state throughout treatment. Studying neuromodulation with multimodal neuroimaging is especially useful for exploring the temporospatial dynamics within functional brain networks (Siebner et al., 2009). Each imaging modality operates according to distinct theories and can provide unique insights. For example, both electroencephalography (EEG) and magnetoencephalography (MEG) sensors are differentially sensitive to the dipole moments that radiate from the brain; EEG sensors are sensitive to normal dipole moments whereas MEG sensors are sensitive to tangent dipole moments (Baillet et al., 2001; Nunez & Silberstein, 2000; Papanicolaou, 2009). Using these modalities along with structural and diffusion MRI can enhance our understanding of regions involved in MDD in the context of the depressive circuit.

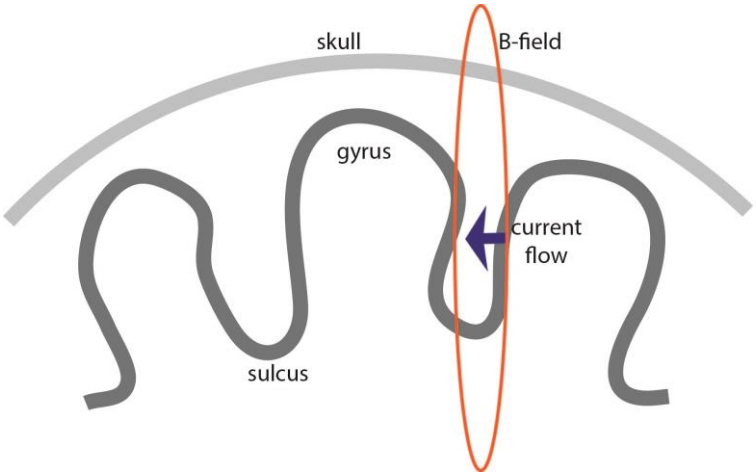

Figure 2.1: Origin of magnetic signals for MEG. Magnetic (B) fields are perpendicular to current flow making MEG sensors more sensitive to current in the sulcus than the gyrus.

II. Functional Connectivity

A thorough analysis of the functional role of distinct regions of the brain and their interactions is necessary to add details to the network model of MDD. Therefore, it is important to understand the concepts of functional segregation (activation of a particular brain area) and functional integration (synchronized stimulation of distant neural networks). Stemming from these concepts are the measures (Sakkalis, 2011; Schoffelen & Gross, 2009) of functional connectivity and effective connectivity. Functional connectivity (FC) is defined as temporal correlation of spatially distributed cortical regions. Effective connectivity (EC) is defined as the direct or indirect influence of one neural assembly on another, which describes directional interactions.

For the purpose of this study, we focus on linear measures of FC. We use the methods of magnitude-squared coherence (coherence), which is the cross-spectral density function of two signals, or wavelet coherence, which requires *a priori* information to determine time-frequency resolution. Coherence is sensitive to power and phase and measures relationship stability; whereas correlation is sensitive to polarity and phase, but

not amplitude. These measures of connectivity are essentially signal processing algorithms and assume stationarity. For increased accuracy, connectivity should be determined by integrating neuroanatomical information from DTI and high temporal resolution approaches (Sakkalis, 2011; Schoffelen & Gross, 2009). Furthermore, studies of white matter variations have further validated the link between cortical excitability and connectivity (Klöppel et al., 2008; Siebner et al., 2009). Physiologically, it is important to note the effects of synaptic plasticity as these are the phenomena that are indirectly inferred through the connectivity analysis. Characteristically, long range interneurons are responsible for temporal synchrony of distant oscillators (Buzsaki, 2006).

III. Computational Analysis

Computational models are another important tool to understand the effects of neuromodulation. Models created for MDD should account for the geometry and properties of the anatomical surface as well as the physics of the stimulation applied. The feasibility of patient-specific models has been displayed in characterizing the effects of DBS in Parkinson's disease (Butson et al., 2007). These models provide an avenue for quantitative estimates of the effect of stimulation. Finite element methods (FEM) are employed to computationally model TMS. Studies show that complex cortical geometry has an effect on the electric field and the current densities that are produced on the cortical surface as a result of stimulation (Thielscher et al., 2011). Moreover, it is imperative to consider the complex biophysical properties of neuron-interneuron architectures as they vary and can be differentially recruited based on firing frequencies of the principal cells (Buzsaki, 2006).

For cortical stimulation, one group (Holdefer et al., 2006) integrated white matter anisotropies with compartmental geometries and resistivities to predict the strength and location of current densities as a function of electrode location on the scalp. The Holdefer et al. model determined that at low stimulation intensities, small areas in white matter may be activated first depending on the dominant fiber orientation in that region. Another study (Wongsarnpigoon & Grill, 2008) investigated the role of electrode polarity in the modeling approach. They showed that the current density and activating function were greatest beneath the stimulating electrode. However, anodes targeted neurons that were oriented perpendicular to the cortical surface, whereas cathodes targeted those that were oriented in a parallel configuration. Wongsarnpigoon and Grill also demonstrated that the magnitude of the activating function was inversely proportional to the thickness of the cerebrospinal fluid (CSF) and dura. The practical application of these models is that several configurations of electrode placements and polarities can be used to selectively activate a region of the cortex.

Computational models also help interpret results from clinical studies and add to our knowledge of the underlying neurophysiology. Amatrudo et al. (2012) observed that structural differences between two neurons accounted for differences in passive properties but not action potential (AP) firing or synaptic response properties. The authors suggest that differences in functional properties at the single neuron level contribute to differences in network behavior. In addition, greater connectivity and dendritic complexity of DLPFC neurons support a high level of cognitive function. These insights can be used to plan and assess stimulation effects of neuromodulation at the MDD circuit.

CHAPTER 3: WHAT IS THE ROLE OF STIMULATION PARAMETERS IN PATIENT RESPONSE TO EPCS FOR MDD?

I. Introduction

The DLPFC is a potential target for EpCS therapy. Neuropsychological and neuroimaging studies have found the DLPFC to be functionally involved in mood disorders (Koenigs & Grafman, 2009; Ressler & Mayberg, 2007). More specifically, the L-DLPFC (Brodmann areas 9/46) is hypoactive in individuals suffering from MDD (Koenigs & Grafman, 2009; Sackeim, 2001). EpCS of the L-DLPFC was recently evaluated in an 11-patient safety and feasibility study (Kopell et al., 2011). This method is considered safer than techniques such as deep brain stimulation (Holtzheimer et al., 2012; Lozano et al., 2008) (DBS) because it does not require penetration of the dura. It is also considered more focal than TMS or vagal nerve stimulation (VNS) because the electrodes are located directly adjacent to the neuroanatomical target region (Nahas et al., 2010).

A wide range of stimulation configurations are available for EpCS. These can strongly affect the strength and orientation of the induced electric field as well as the specificity of the neurons that are recruited (Nahas et al., 2010). The stimulation parameters (frequency, amplitude, pulse width) and the electrode contact locations are expected to be cofactors for the overall effectiveness of the treatment (Fregni et al., 2006; Lefaucheur, 2008). The orientation of the dendrites and axons in the induced electrical field further influences the direction of the polarizing effect (Lefaucheur et al., 2008; Manola et al., 2007). These orientations are highly correlated with a specific location on the cortical surface. An rTMS study (Herbsman et al., 2009) for depression over the

prefrontal cortex was conducted to validate the differential effects of location within the DLPFC. Herbsman et al. found a linear relationship between coil placement and the Hamilton Depression Rating scale (Hamilton, 1960) (HDRS-28) improvement. These findings illustrate the complexity associated with EpCS and the treatment of depression in terms of electrode location and stimulation protocol.

A recent study reported on the feasibility of EpCS of L-DLPFC for the treatment of MDD (Kopell et al., 2011). Data from that previous trial were analyzed further as part of our current study to understand the degree to which stimulation parameters and electrode location were predictors of clinical response. The objective of this study was to estimate the degree of variability in HDRS-28 that is attributable to changes in stimulation protocol. In particular, the goals of this study were: 1) Determine whether changes in the stimulation protocol, which consisted mainly of varying anode/cathode configurations, had a differential effect on HDRS-28 2) Estimate the time necessary for treatment to elicit a robust clinical response; and 3) Explore the effects of stimulation location on clinical outcome.

II. Methods

Participants

Data from eleven subjects (6 males, 5 females) with recurrent MDD without psychotic features were analyzed. The inclusion criteria for these patients have been described in a previous report (Kopell et al., 2011). Approval from the Institutional Review Board at the Medical College of Wisconsin was obtained prior to conducting the analysis.

Study Design

Participants were randomly assigned to either 8 weeks of an initial sham period (n = 5) or active stimulation (n = 6). Patients in the sham group received active stimulation after the initial 8-week period. The stimulation study duration was 104 weeks with periodic assessments using HDRS-28 (primary outcome), and the following secondary outcomes: Montgomery-Asberg Depression Rating Scale (MADRS), Global Assessment of Functioning (GAF), and Quality of Life Enjoyment and Satisfaction Questionnaire (QLES). For the present analysis, only the HDRS-28 scores were used.

Stimulation was applied using a two-electrode implantable paddle with platinum-iridium contacts in the L-DLPFC. Electrode contacts were 3.75 mm in diameter and 15 mm apart. They were implanted over the posterior half of the middle frontal gyrus. The implantable pulse generator (IPG), which was implanted in the sub-clavicular region, delivered continuous stimulation as specified by the stimulation protocol. Patients received repeated clinical evaluation during the study period. Clinical response was defined as 40% improvement from baseline HDRS-28 scores. Remission was defined as an HDRS-28 score of less than 10.

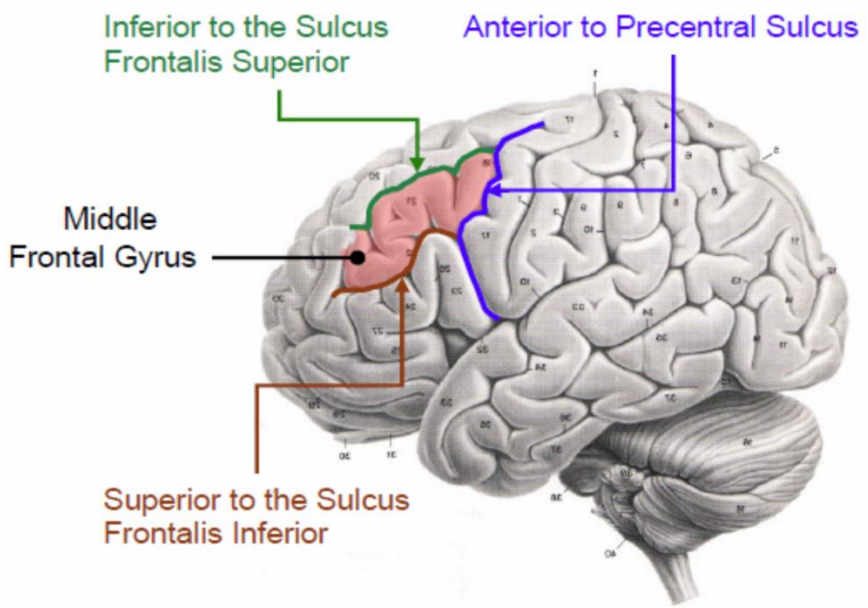

Figure 3.1: Site of 2-electrode paddle implant in the L-DLPFC. This figure was reprinted with permission from Kopell et al. Neurosurgery (2011)

Stimulation Settings

The IPG used in this study was capable of providing a range of stimulation modes that differed in polarity (anode or cathode), duty cycle (percentage of pulses that were active), and number of active contacts (one or two). Eight different stimulation modes were applied during the study. Each patient began with monopolar, anodal stimulation at 50 Hz, 150μs pulse width (PW), and 6.5mA of total current. The first stimulation mode applied was Q03. In this mode both the anterior and posterior electrodes were anodic and the current was divided between them (3.25mA at each electrode). All patients were stimulated using this mode for the first 8 weeks of active stimulation. If this mode was effective, then other modes at reduced power were tried. First, modes Q29 (50% duty cycle of Q03) or Q28 (25% duty cycle of Q03) were tried to preserve effectiveness while simultaneously prolonging IPG battery life. If these modes failed to show an improvement, then the patient was switched to mode Q21, which provided unipolar

stimulation where the polarity toggled between anode and cathode in a pseudorandom manner. During this mode, output polarity was set to one of the four unipolar configurations every second where either electrode could be anodic, cathodic, or off. Because only one of the leads was active, all current (6.5mA) was delivered through the active electrode contact. Similar to Q03, if this mode was effective then the patient was switched to a lower power setting with mode Q37 (50% duty cycle of Q21) or Q36 (25% duty cycle of Q21) in an effort to extend IPG battery life. If none of these modes were effective, the clinician selected another appropriate setting. During the study, modes Q09 (75% duty cycle) and Q12 (50% duty cycle) were administered occasionally. Both modes were characterized as anodic stimulation modes at decreased power. All modes were categorized in three groups: anodic at full power (Q03), anodic at reduced power (Q28, Q29, Q09, Q12), and mixed polarity (Q21, Q36, Q37).

Data Analysis

A cumulative incidence curve was calculated using the Kaplan-Meier survival algorithm to characterize the time necessary to observe a clinical effect of the treatment. The effect of stimulation mode on HDRS-28 over time was modeled via a piecewise linear mixed model. The baseline score and the slope of the change in HDRS-28 during each intervention mode (anodic full power, anodic reduced power, and mixed polarity) were included both as fixed and random effects. Thus, we could estimate the average over subjects while allowing for between-subject variability and incorporation of repeated measurements per subject. The change-points of the model were not estimated; the subject-specific times of mode change were used instead. The model was fitted using Proc Mixed in SAS 9.2 (SAS Institute, Cary NC).

Two graphs were generated from the fitted model. The first graph shows observed and predicted HDRS-28 trajectories for each patient over time with model-based 95% confidence intervals. According to the model, a particular mode within a patient had the same slope for each episode. The second graph shows the observed and fitted values of HDRS-28 change within each contiguous episode using the same mode; the value at the last observation of a previous mode has been subtracted from each observation at the subsequent mode.

Stimulation Location

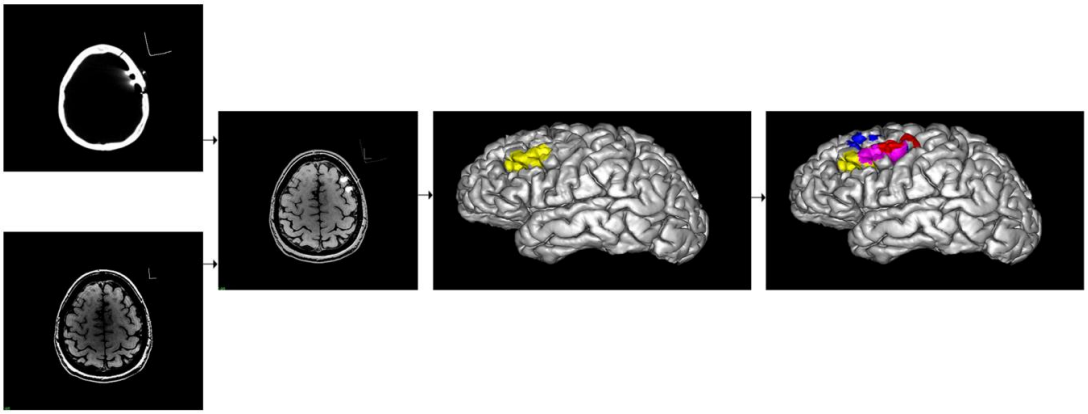

Figure 3.2: A flowchart describing the process used to determine the stimulation location. Imaging data for 4 subjects who were enrolled at the Medical College of Wisconsin were used to assess the effect of location on clinical outcomes. The presurgery MRI and postsurgery CT scans were co-registered to determine the site of implanted electrodes. The pial surface for each subject was then extracted via FreeSurfer (Martinos Center for Biomedical Imaging). The stimulated region of interest (ROI) was defined as a locus of points on the pial surface within a 1-cm radius of each electrode. Each patient ROI was then mapped to one patient brain for comparison.

The study protocol required the electrodes to be placed on the L-DLPFC (Figure 3.1). Imaging data for 4 subjects who were enrolled at the Medical College of Wisconsin were used to assess the effect of location on clinical outcomes. The preoperative magnetic resonance imaging (MRI) and postoperative computed tomography (CT) scans were fused using Analyze version 10 (AnalyzeDirect, Lenexa, KS) to determine the site

of the implanted electrodes. The pial surface for each subject was then extracted from the preoperative MRI via FreeSurfer (Martinos Center for Biomedical Imaging). A stimulated ROI, calculated and displayed using MATLAB (Mathworks Inc, Natick, MA) and SCIRun (Center for Integrative Biomedical Computing, University of Utah), was defined as a locus of points on the pial surface within a 1-cm radius of each electrode. The analysis for mapping the ROI did not take into account the difference between anodic and mixed stimulation. However, a quantitative comparison of the effects of stimulation polarity and location in between-subjects and within-subjects data is essential and should be addressed in future studies. Each patient ROI was then mapped to one patient brain, which served as an atlas brain, for comparison (Figure 3.2). The ROI for each patient was saved as a matrix of node values. These nodes were then mapped to the atlas brain using a template-matching algorithm in FreeSurfer. Lastly, the nodes were color coded in SCIRun based on maximum percent improvement observed in HDRS-28.

III. Results

Stimulation Effectiveness Varied as a Function of Mode and Duration

Eleven patients were assessed over the course of 104 weeks. For the present analysis, all patients (active and sham) were normalized so that baseline (Week 0) was the point at which stimulation was turned on. Stimulation effectiveness as a function of duration and mode are shown in a piecewise linear mixed model for each subject (Figure 3.3). Clinical response was defined as a 40% reduction in the HDRS-28 score from baseline. Eight subjects (Patients 1-8) were responders under this criterion. The linear models for each mode were grouped to their respective categories (anodic full power,

anodic reduced power, and mixed polarity) (Figure 3.4). A statistically significant improvement in HDRS-28 was observed during the application of anodic full power modes (slope = -0.109, $p = 0.034$). A statistically significant effect was also observed during the application of mixed polarity modes (slope = -0.26, $p < 0.001$). However, improvement during anodic reduced power modes did not reach significance ($p > 0.05$). Lastly, improvement during the initial 8-week period contributed greatly to the effect of anodic modes at full power (Figure 3.5).

Response Probability Increased Over Time

A Kaplan-Meier curve was used to determine the time necessary to observe a clinical effect of the EpCS (Figure 3.6). Analysis of the baseline HDRS-28 showed that it had no predictive effect on the time of response ($p = 0.63$). Over 50% of the responses (5 of 8) occurred within the first 20 weeks of the study as shown in Figure 3.3. In comparison, only three subjects displayed a clinical response at eight weeks, which was the end-point in the clinical trial. These results were generated using a 40% improvement threshold. When the response probability was evaluated with a threshold of 50% improvement from baseline, the results were similar. By week 20, 50% of the responses (3 of 6) had occurred.

Stimulation Effectiveness Was Location-Dependent

An average value for the maximum improvement from baseline HDRS-28 was calculated at each of the nodes that were mapped in the ROI. The improvement ranged from 52%-93%. Nodes in the medial and posterior areas correlated with lower improvement values (red) whereas those in the lateral and anterior areas correlated with higher improvement values (blue). This result suggests a trend that stimulation in the

lateral and anterior region of the L-DLPFC correlates with better clinical outcomes (Figure 3.7). It also illustrates a subregion within the L-DLPFC that could serve as a target for future therapies.

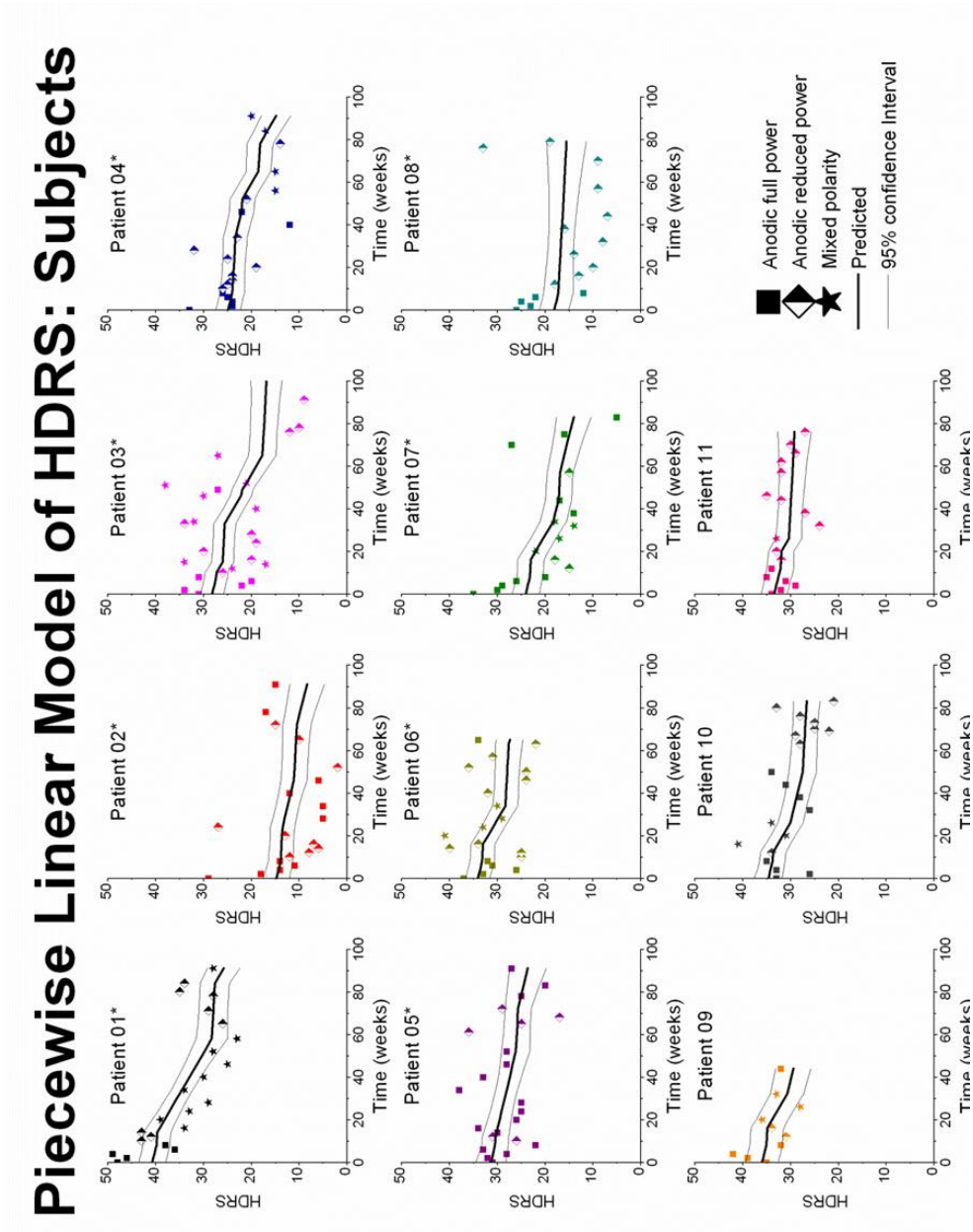

Figure 3.3: Piece-wise linear mixed model for each patient based on stimulation mode. Each contiguous episode of a stimulation mode within a patient was linearly modeled. Of the 11 subjects, 8 were clinical responders over the course of 104 weeks.

*Patient reached criteria for clinical response during the 104-week study period.

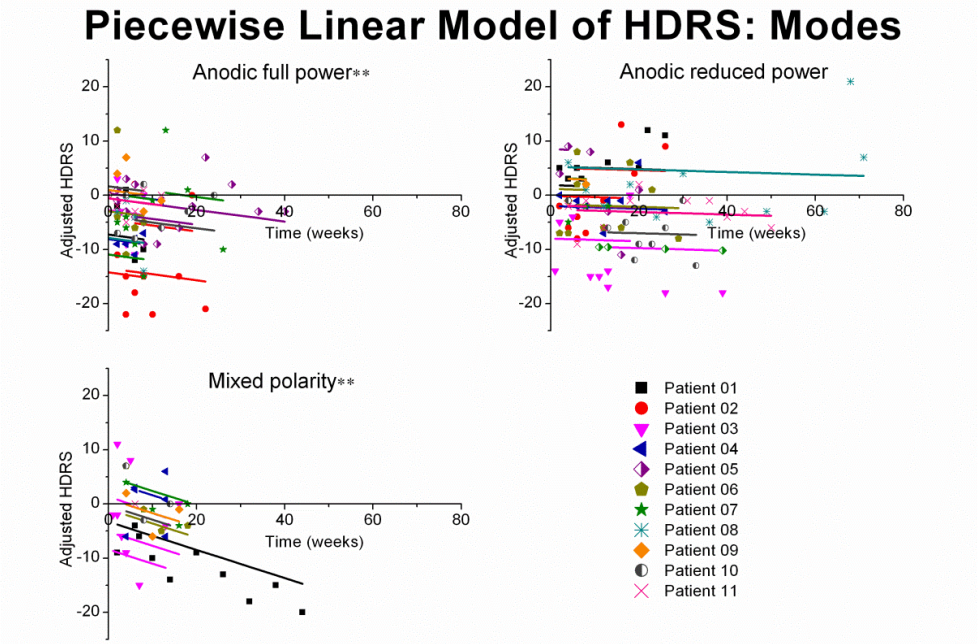

Figure 3.4: Piecewise linear mixed model for each mode. The slopes obtained for each contiguous stimulation mode as displayed in Figure 3.2 were grouped to study the effect of stimulation parameters. The improvement in HDRS-28 during the application of the anodic mode at full power was statistically significant (slope = -0.109, $p = 0.034$). Improvement in HDRS-28 during the mixed mode was also statistically significant (slope = -0.26, $p < 0.001$). However, anodic modes at reduced power did not have an effect on HDRS-28 ($p>0.05$). **Modes showed statistically significant improvement

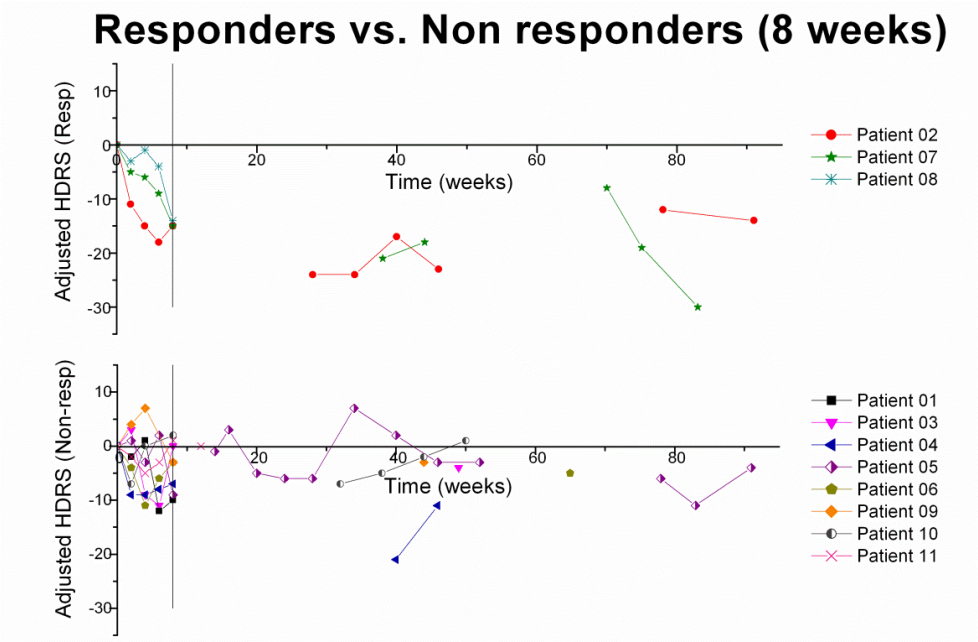

Figure 3.5: Responders versus nonresponders at 8 weeks. The effect of anodic mode at full power at initial versus later time points in both responders and nonresponders. The data shown are for responders (top panel, n = 3) and nonresponders (bottom panel, n = 8) during the initial 8 weeks of stimulation. The vertical lines in each plot indicate the initial 8-week period. Responders improved dramatically in the initial period and may have experienced a floor-effect, which limited further improvement.

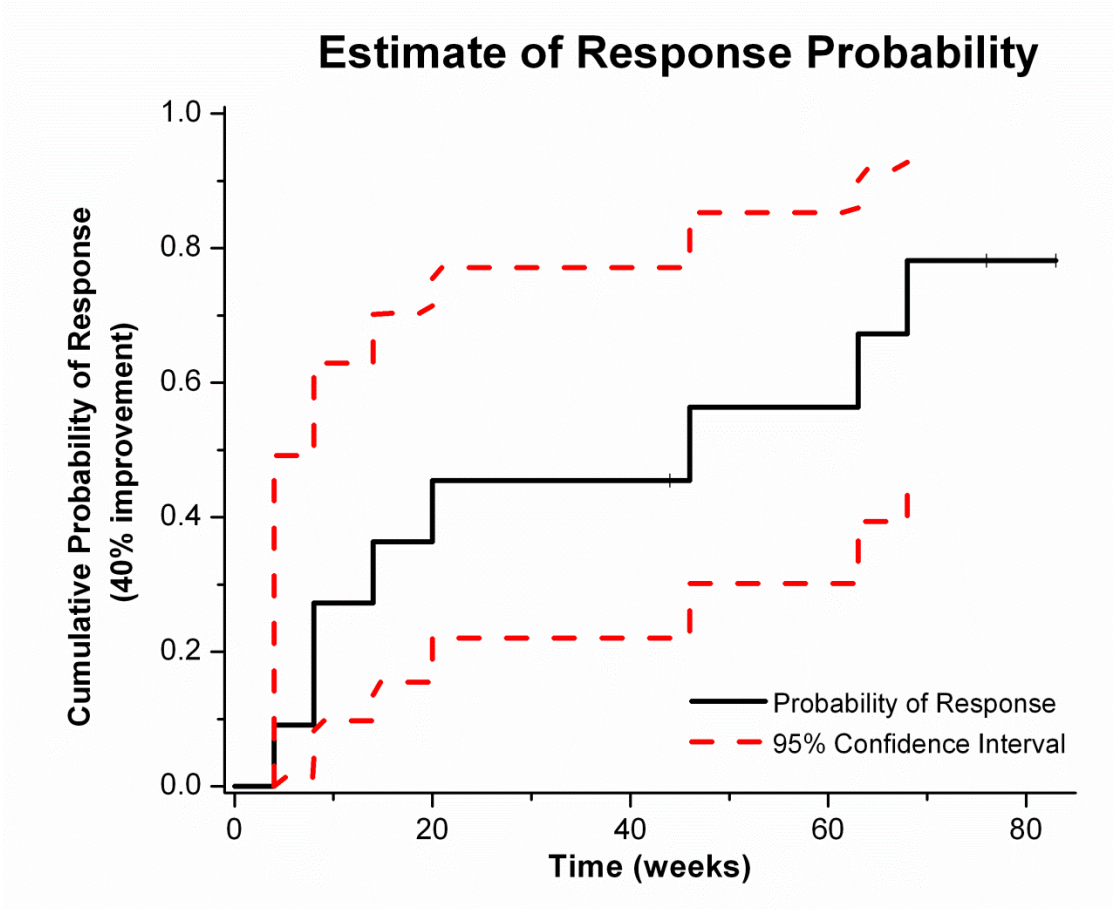

Figure 3.6: Kaplan-Meier estimate of response probability. Each step in the solid black line indicates that one or more patients reached the response criterion.

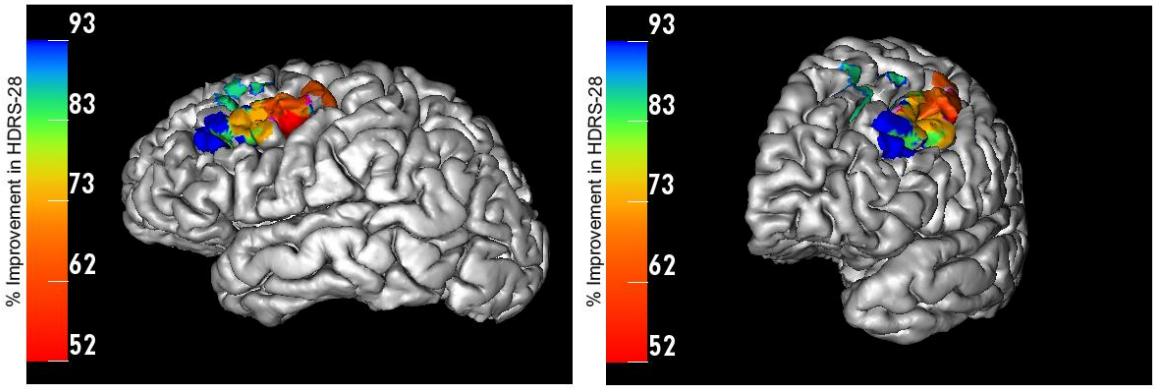

Figure 3.7: Stimulation in the lateral and anterior region of the L-DLPFC correlates with better clinical outcome. An average value for the maximum improvement from baseline HDRS-28 was calculated at each of the nodes that were mapped in the ROI. Improvement ranged from 52%-93%. Nodes in the medial and posterior areas were correlated with lower improvement values (red) whereas those in the lateral and anterior areas were correlated with higher improvement values (blue).

IV. Discussion

The goal of this study was to assess the degree of variability in HDRS-28 due to changes in stimulation protocol or electrode location. In particular, the aims of this study were to determine if changes in the stimulation protocol (anode/cathode) had a differential effect on HDRS-28, to estimate the time necessary for treatment to evoke a clinical response, and to explore the effects of stimulation location on clinical outcome.

Based on the effects of cathodal and anodal stimulation (Fregni et al., 2006; Lefaucheur et al., 2008), we expected the mixed polarity modes to have a minimal effect. Contrary to this theory, the results indicated a significant effect of the mixed mode on the improvement of HDRS-28. One reason for this effect could be the magnitude of the current delivered. Current delivery was more focused in the mixed mode because only one contact was active at a time during stimulation and therefore all of the current (6.5mA) was delivered through that electrode. Also, anodes and cathodes are selective in which neural elements are excited. Because the mixed polarity modes allowed for each electrode to serve as an anode and a cathode, a wider range of neural elements may have been recruited. Lastly, the direction of the activation is influenced by the orientation of dendrites and axons in the induced electrical field (Lefaucheur et al., 2008). The improvement due to mixed mode application could be attributed to the neuron orientation(s) underneath the cortical surface. This claim could be further investigated by exploring the effects of selective stimulation on the longitudinal outcomes of other neuromodulation techniques such as rTMS (see Chapter 4) that allow for control of the electric field orientation relative to cortical tissue.

The results demonstrate that improvement was also significant with the anodic full power modes. The effect of the anodic full power modes was observed mostly in the initial period (8 weeks), and in some patients most of the improvement was achieved during this period. Therefore, due to a floor-effect, other modes may have been unable to further improve the response (Figure 3.5). When looking closely at the data, the subjects can be divided into fast versus slow responders. The floor-effect could be observed in the fast responders. Ideally, a statistical comparison of anodic full power modes applied initially versus later in the study would provide more perspective. However, due to limited data points for the latter condition, this analysis was not possible. A similar trend was observed for HDRS improvement in a DBS study for MDD during the initial 2 months of treatment (Lozano et al., 2008). It is also essential to note the effects of duty-cycle on clinical outcome since discontinuous stimulation may have an impact on the long-term sustainability of treatment (Nahas, 2010). However, according to our results, the intermittent stimulation, which was characterized by a lower duty cycle (anodic reduced power), was not effective.

The time course for response to EpCS was variable, which could result from many factors including characteristics of the patient, life events that occurred during the study period, stimulation location, and stimulation protocol (including mode). There are periods of improvement in individual patients during which the stimulation protocol was fixed and the HDRS-28 scores declined steadily over several weeks. Hence, the data suggests that therapeutic response is due to some type of plasticity brought about by chronic stimulation. Cortical excitability is modulated by altering resting potential during stimulation and by modifying synaptic transmission (Boggio et al., 2008; Liebetanz et al.,

2002). Also, the neurochemical and neuroendocrine processes that are responsible for expression of secondary messengers are time consuming and complicate the programming algorithms necessary to observe efficacy in EpCS (Lefaucheur et al., 2008). When considering the results of different stimulation modes, it is important to note the possibility of metaplasticity. Metaplasticity is a term used to describe the changes that occur in plasticity due to neuronal influences from previous treatments steps and medications. This phenomenon can influence subsequent changes in plasticity and affect both response and relapse.

MDD is widely accepted to be heterogeneous (Krishnan & Nestler, 2008) and, therefore, patient response rates inherently vary. A recent pharmacological study, Sequenced Treatment Alternatives to Relieve Depression (STAR*D) trial (Rush et al., 2006), concluded that remission rates decrease with an increase in the number of acute treatment steps. Despite the longer amount of time taken by some of the subjects to reach remission, the study noted that remission was associated with better prognosis even when achieved after numerous treatment steps. Thirty-five percent of patients with MDD required more than eight weeks to reach remission with their first antidepressant. This conclusion further emphasizes that physiological change necessary to cause and sustain improvement occurs at different rates in different individuals. The results of our response probability analysis suggest that in order to observe a clinical response in over half the responders, the treatment outcome should be evaluated at 20 weeks instead of 8 weeks. In another recent EpCS study (Nahas et al., 2010), average improvement in HDRS-24 was about 36% from baseline at 16 weeks whereas at 28 weeks the average improvement increased to 55% from baseline. These findings further support our results.

L-DLPFC plays a major role in neuropsychological disorders and tends to be hypometabolic in MDD. To evaluate the effects of location on stimulation, a transcranial direct current stimulation (tDCS) study (Boggio et al., 2008) compared stimulation at the prefrontal cortex with an active control group that was stimulated at the occipital cortex. At the end of the Boggio et al. study, there were a significantly greater number of responders in the active treatment group than in either the sham or the active control group. However, L-DLPFC defines a fairly broad area and stimulating at this target is still imprecise. It is unclear where electrodes should be placed during EpCS in order to maximize efficacy of the treatment. The last analysis in this study was aimed at exploring the effects of stimulation location on clinical outcome. Our data suggests a trend in which stimulating in the anterior and lateral regions of the L-DLPFC is more efficacious than in the posterior and medial regions (Figure 3.7). This finding is significant as it emphasizes the importance of stimulation location. With an anterior and lateral placement of the electrode, the stimulation is more likely to be in an effective region of the DLPFC. In a rTMS study for depression (Herbsman et al., 2009), 54 patients were stimulated over the prefrontal cortex for 3 weeks. Herbsman et al. found a linear relationship between coil placement and HDRS improvement. According to their results, there was a 5 mm difference in the average coordinate position of the non-responders and the responders in all three axes (x, y, z). They were unable to observe the same dependence on the coil position in the placebo group. Likewise, they also concluded that stimulating lateral and anterior in the DLPFC was associated with better clinical response.

V. Conclusions

In general, clinical trials are designed to tightly control treatment such that outcome variability is attributed to differences among patients in the study cohort. However, neuromodulation therapies such as EpCS have many additional sources of variability including electrode location and stimulation protocol. The methods used in this study confirm that quantitative comparison of stimulation among different patients can be accomplished by a pipeline of analysis tools. The results of our study contribute largely to the understanding of EpCS. We also believe that this approach can inform many types of neuromodulation studies by first quantifying where and how individual patients were stimulated, and second by correlating stimulation location with effectiveness. Importantly, we believe that this approach can provide insights whether or not a study reached its therapeutic objectives.

CHAPTER 4: WHAT FUNCTIONAL CHANGES RESULT FROM rTMS FOR MDD?

I. Introduction

Due to the heterogeneity of MDD, about a third of the patients suffering from the disorder are resistant to pharmacological antidepressants and/or psychotherapy. Neuromodulation therapies have emerged as potential treatments for depression. As described previously, DLPFC and VMPFC are two of the main targets of neuromodulation therapy. DBS at the sACC of the VMPFC network has shown promising results with inhibitory stimulation (Hamani, Diwan, Isabella, et al., 2010; Hamani et al., 2011; Holtzheimer et al., 2012; Lozano et al., 2008; Mayberg, 2009; Mayberg et al., 2005). Similarly, excitatory, noninvasive stimulation at the DLPFC via rTMS has efficaciously ameliorated depression for patients in several studies (Downar & Daskalakis, 2013; Fitzgerald et al., 2009; Herbsman et al., 2009; O'Reardon et al., 2007). Lesion studies and advances in neuroimaging have provided evidence of the role of PFC in depression. First of all, these two targets exhibit opposite metabolic activity in the pathological depressed state (VMPFC: hyper, DLPFC: hypo) (Koenigs & Grafman, 2009; Pathak et al., 2012; Ressler & Mayberg, 2007). We applied rTMS at the DLPFC because it is superficial enough to access noninvasively and still plays a major role in higher cognitive functions and affective regulation.

We used resting-state MEG to assess the longitudinal changes that resulted due to high-frequency rTMS therapy. MEG is a functional neuroimaging method that senses magnetic fields generated by neural activity. Specifically, these recordings represent the sum of thousands of synchronous postsynaptic currents in pyramidal neurons (Figure

2.1). Choosing MEG over fMRI or EEG for this study is fitting due to its excellent millisecond-level temporal resolution and the reliability of fields that are less distorted due to the skull and the scalp allowing for a more robust analysis at the source level to characterize regional activity as well as connectivity based on time-dependent measures (Baillet et al., 2001; Gross et al., 2013). Recent studies have investigated TMS as both a priming method and a treatment option for depression (Herbsman et al., 2009; Nahas et al., 2001; O'Reardon et al., 2007). Location of stimulation and intensity, which is determined based on RMT, are important parameters in rTMS therapy.

Efficacy of rTMS therapy in treating MDD has previously been established and is not the focus of this study. Rather, the current study aims to identify objective indicators of antidepressive response to rTMS using functional neuroimaging. The long-term goal is to determine which patients will respond to anti-depressive treatment and to customize neuromodulation therapy accordingly. We are interested in two primary questions: 1) Which depressive circuits previously targeted for DBS are modulated during successful rTMS therapy for MDD? 2) Can changes in functional connectivity predict clinical response? Our hypothesis is that modulation of the L-DLPFC will be reflected through longitudinal changes in the power spectrum of MEG results and changes in functional connectivity with other targets of the depressive circuit.

II. Methods

rTMS delivery

High frequency (10 Hz) rTMS was administered to the L-DLPFC (Brodmann areas 9 and 46) in five MDD patients (n=5) according to an IRB approved protocol. A

total of 1000 biphasic pulses were delivered in 25-second cycles (5 seconds on, 20 seconds off) over 20 trains per session using a Magstim Rapid stimulator (Magstim Company Limited, Whitland, UK). Treatment was delivered for five 15-minute sessions per week over four weeks. Stimulation was applied at 110% of RMT, which was determined by stimulating the hand-knob of motor cortex. Periodic behavioral assessments were performed with the Montgomery-Asberg Depression Rating Scale (MADRS).

Anatomical Imaging

High-resolution (3T) structural MRI was acquired before treatment to assist with targeting and navigation. It was used for 3D reconstruction of the head volume (scalp, skull, cortex) using FreeSurfer (Dale et al., 1999) (Martinos Center for Biomedical Imaging) and Brainstorm (Tadel et al., 2011). The ANT neuro-navigation system was used for accurate real-time targeting, and to record the position and orientation of the TMS coil during each pulse (+x towards the nose, +y towards the left ear, and +z in the superior direction with the origin at the center of the head) (Figure 4.1).

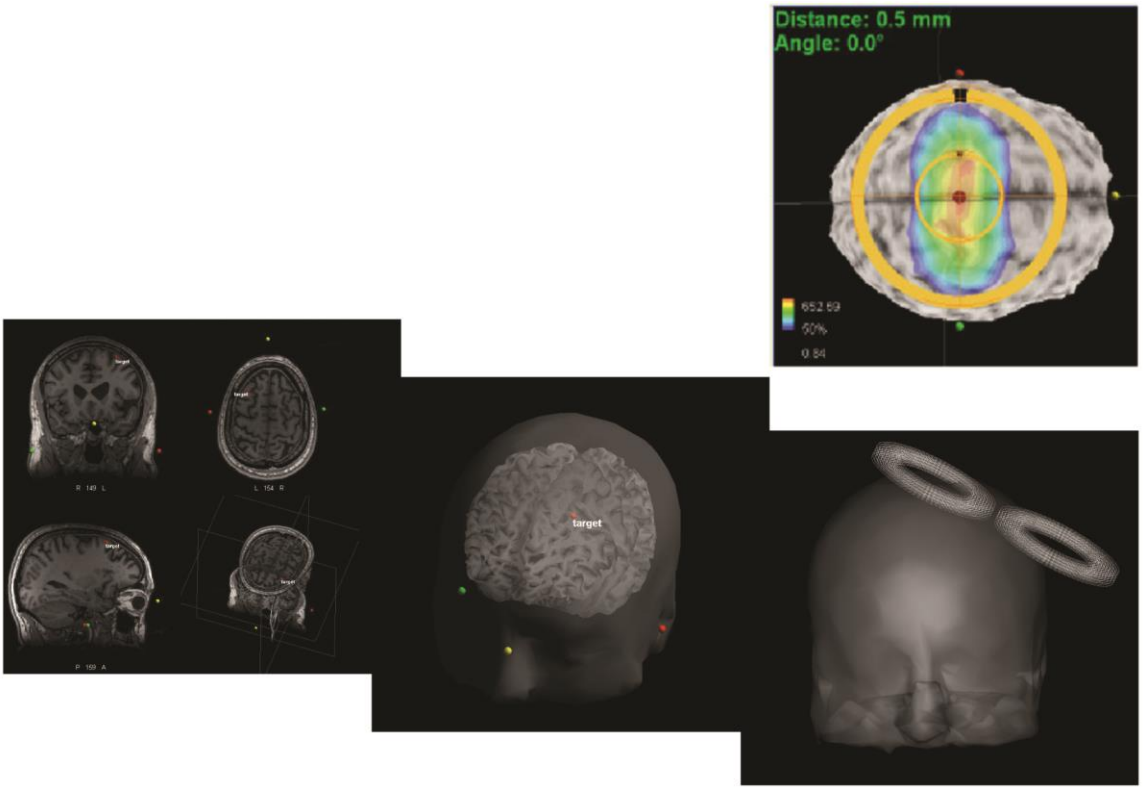

Figure 4.1: Neuronavigation for rTMS therapy. Subject-specific MRI was used for 3D reconstruction of the head volume. High-frequency rTMS (10Hz) at 110% of the RMT was then applied at the L-DLPFC with real-time targeting using the ANT neuro-navigation system.

Functional Imaging

MEG was recorded at 1024 Hz using a 306-channel VectorView system (Elekta Neuromag Ltd, Helsinki, Finland). EOG and EKG were also recorded simultaneous to MEG for post-hoc artifact removal. MEG was acquired at four time points: before treatment, halfway through the treatment course (2 weeks), at the end of the treatment course (4 weeks), and two months after the end of treatment. Empty-room recordings were also collected at these acquisitions to use for noise modeling. During MEG, the subject was in the supine position with sensors positioned above the head. A total of 24 minutes of data was collected in four 6-minute runs. Each condition (eyes-open and eyes-closed) was repeated once.

Source Analysis

MEG data for the eyes-closed condition were analyzed for cortical source modeling, power spectral density (PSD), and functional connectivity using Brainstorm (Tadel et al., 2011). The results were assessed to identify longitudinal changes in PSD over standard frequency bands of ongoing oscillatory neural activity. Continuous signals were cleaned with the signal-space separation (SSS) method (Taulu et al., 2005) and further corrected with the signal-space projection (SSP), a method based on principal components analysis to eliminate artifacts caused by eye-blinks and heartbeats, all using default settings in Brainstorm. The data was further processed with a 60-Hz notch filter and a 2-Hz high-pass filter to remove residual noise due to the power line and effects of the DC offset.

The weighted minimum-norm estimate (wMNE), a subtype of distributed source models, was used to generate the source image maps (Eq 3-6), with default imaging parameters in Brainstorm. Elementary dipole current sources were constrained perpendicularly to the individual cortex; additive sensor noise was modeled with a Gaussian distribution with known covariance statistics estimated from empty-room recordings. The Welch periodogram (Eq 7-8) was used to obtain the PSD of each individual source time series on the cortex. Signals from the L-DLPFC were averaged to determine the power at that region. For this analysis, L-DLPFC was defined based on the Desikan-Killiany atlas (Desikan et al., 2006) from FreeSurfer. A linear regression analysis was performed in MATLAB (Mathworks Inc, Natick, MA) to determine if power within a particular frequency band was correlated with clinical improvement. Data was grouped in time (baseline, midpoint, endpoint, follow-up) and a t-test was conducted

between the four slopes to determine if there was a significant linear correlation between power in L-DLPFC and MADRS.

Functional Connectivity

Coherence measures (Eq 9) were used to determine functional connectivity between L-DLPFC and several regions previously investigated for DBS therapy: pregenual anterior cingulate cortex (pACC) and sACC, NAc, and amygdala. The Desikan-Killiany atlas (Desikan et al., 2006) from FreeSurfer was used to define the ROIs. For our connectivity analysis, a sub-region of the L-DLPFC was defined as a 30-cm^2 area. This value for the patch of cortex was approximated based on previously developed computational models that showed the extent of where the most excitable neurons were (Goodwin Dissertation 2014). Once again, data was grouped in time and a regression analysis similar to that of PSD was conducted to determine if there was a significant linear correlation between coherence (L-DLPFC/ROI) and MADRS In addition, a cluster analysis was conducted in MATLAB and visualized in SCIRun (Center for Integrative Biomedical Computing, University of Utah). For this analysis, each node on the L-DLPFC surface was assigned a mean connectivity score based on its coherence with the signals at all nodes in the ROI. A colormap was then used to visualize the differential effects of sub-regions in the L-DLPFC.

III. Results

Data from four responders and one non-responder were analyzed in this study. Clinical response was defined as 40% reduction in MADRS scores from baseline. Stimulation was applied to the L-DLPFC using a predefined target coordinate on an

anatomical MRI. Within the FreeSurfer-defined L-DLPFC, placement of the stimulation target did not differ between subjects. By midpoint, an improvement in depressive symptoms was observed in responders (Table 4.1). These responders continued to improve during treatment and were still in remission at follow-up (Figure 4.2).

MADRs scores over the course of rTMS for depression					
	Dep01 (R)	Dep02 (NR)	Dep04 (R)	Dep05 (R)	Dep06 (R)
Baseline	26	20	24	26	34
Midpoint	6	22	17	17	16
Endpoint	4	28	10	10	5
Follow-up	10	28	8	7	2

Table 4.1: Summary of MADRS scores for all subjects over 4 weeks of rTMS therapy and at 12-week follow-up (R=Responder; NR=Non-responder)

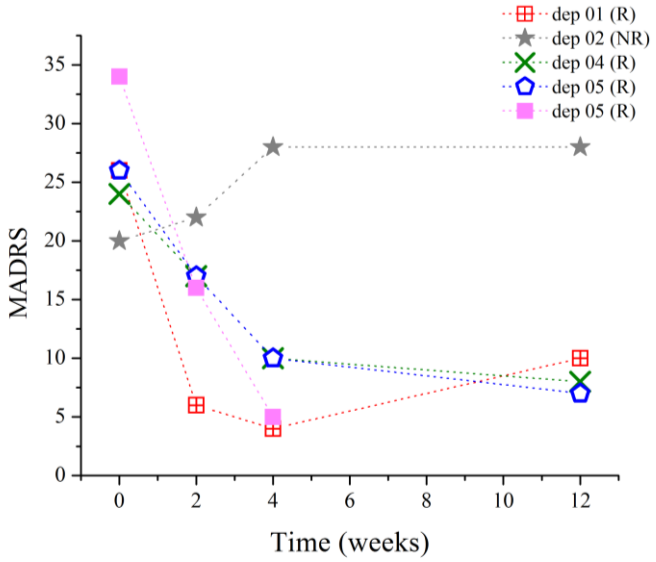

Figure 4.2: Relationship between MADRS scores and time. It is apparent from this plot that drastic improvement occurred in responders during the course of treatment which persisted at least for another eight weeks as demonstrated by the scores at follow-up.

Increase in high-frequency power at the L-DLPFC correlates with an improvement in depressive symptoms

The results from the PSD analysis indicated that an increase in ongoing gamma (γ) (30-59 Hz) power at the L-DLPFC significantly correlated ($p(\gamma) = 0.02$) with an

improvement in depressive symptoms. A power distribution over cortical maps (Figure 4.3) showed a marked increase bilaterally in the frontal regions for responders throughout the course of treatment. These observations were corroborated by a linear regression analysis (Figure 4.4).

A: Changes in Delta Power over the Cortical Surface

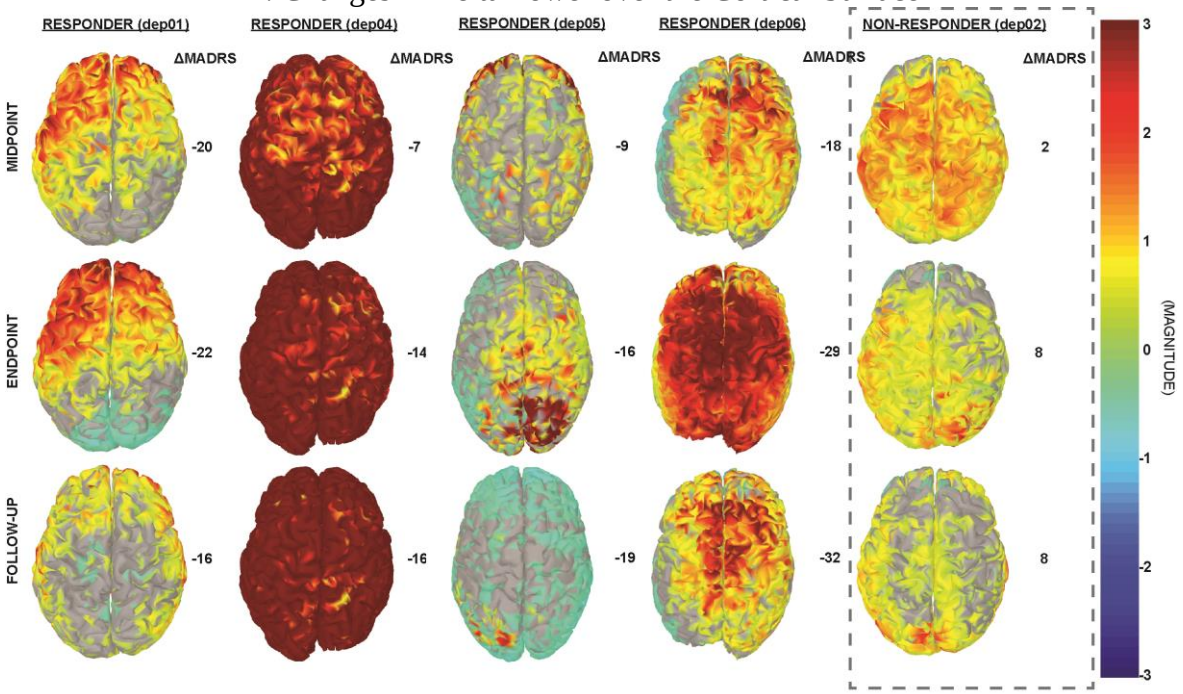

B: Changes in Theta Power over the Cortical Surface

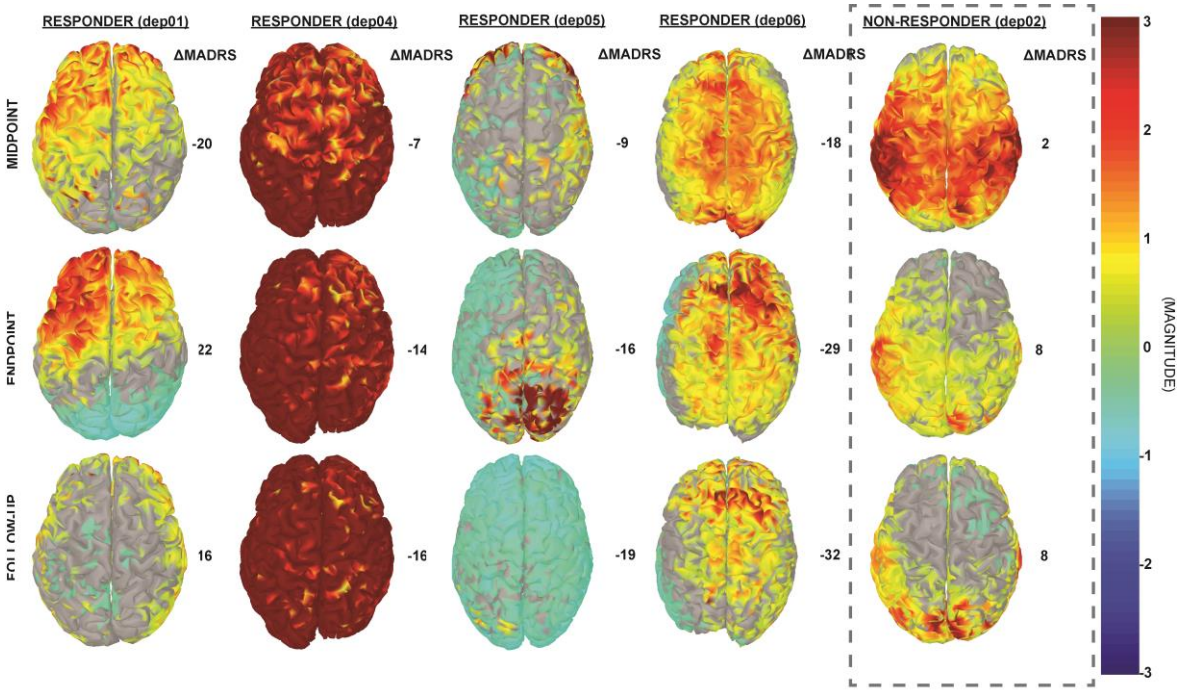

C: Changes in Alpha Power over the Cortical Surface

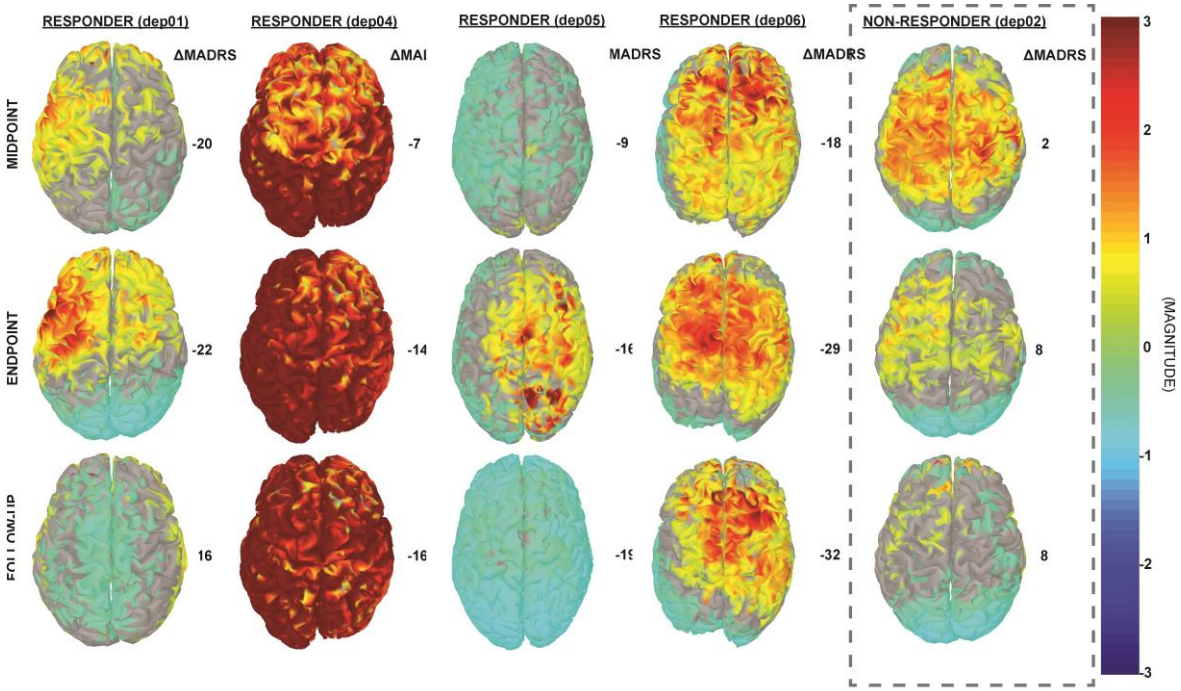

D: Changes in Beta Power over the Cortical Surface

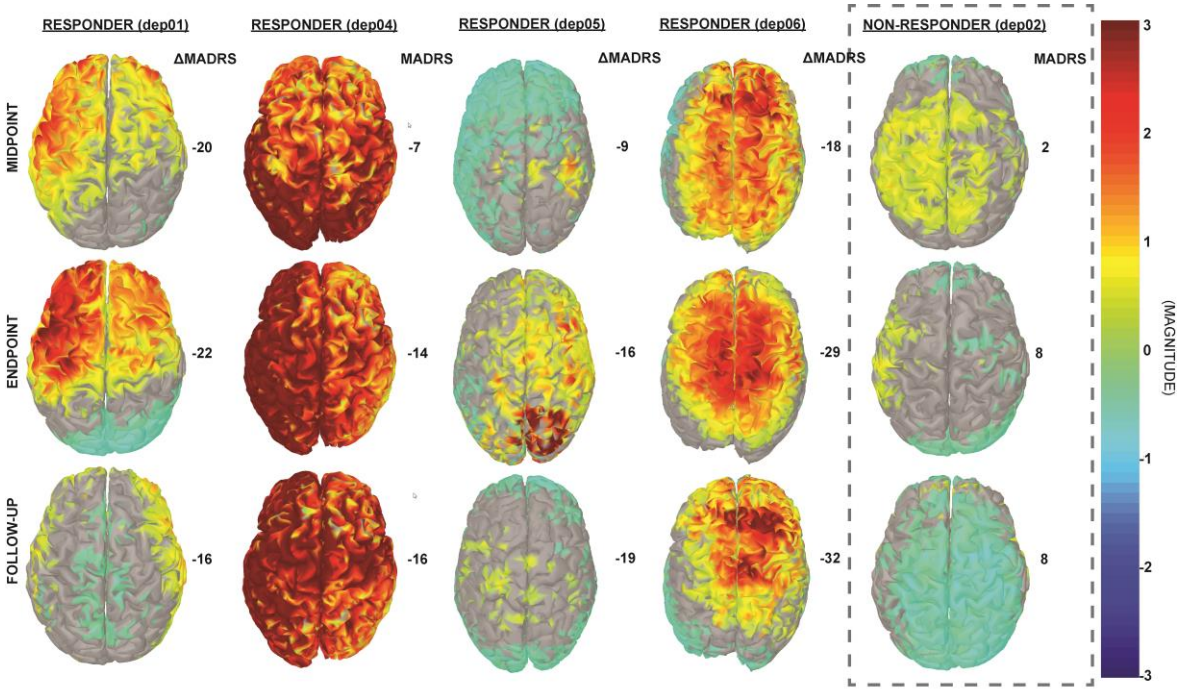

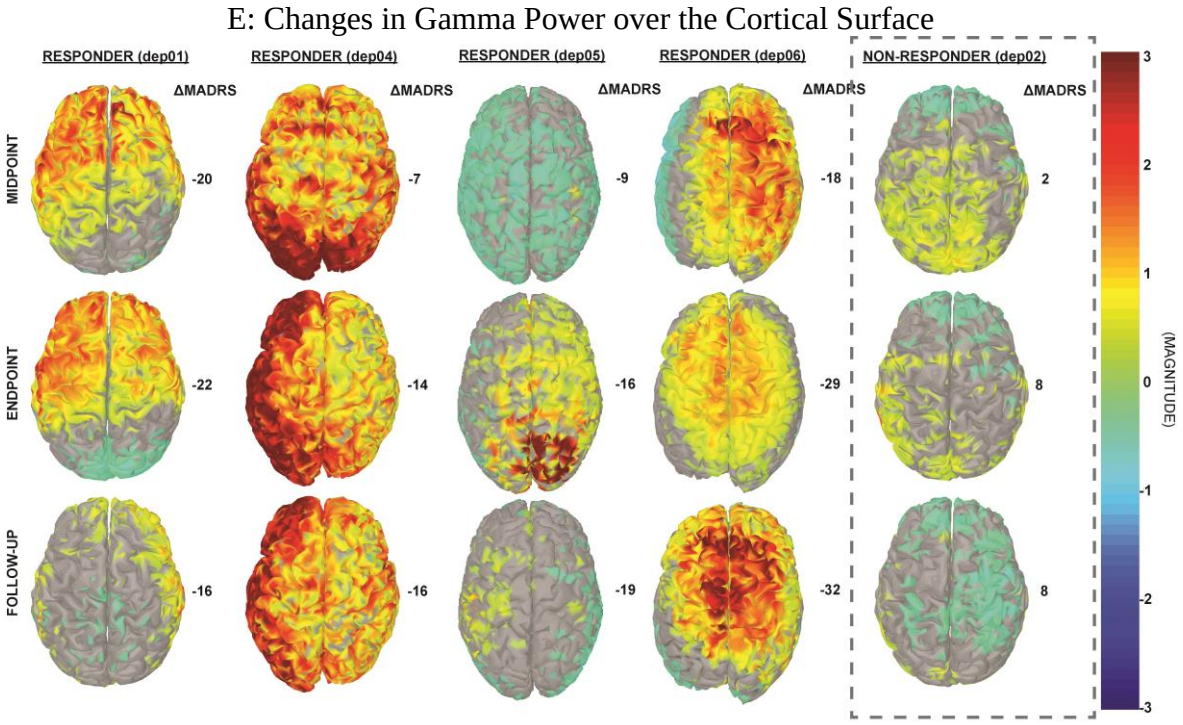

Figure 4.2: Changes in power spectral density (PSD) in source space. These cortical maps display the normalized difference in PSD from baseline in standard frequency bands (delta (A), theta (B), alpha (C), beta (D), and gamma (E)). For the responders, there is a marked increase in high-frequency power (E: gamma) bilaterally in the frontal regions, which corresponds to their improvement in depressive symptoms as determined by the change in MADRS (right column for each patient). A similar trend, specific to the responders, is not observed in the lower frequency bands.

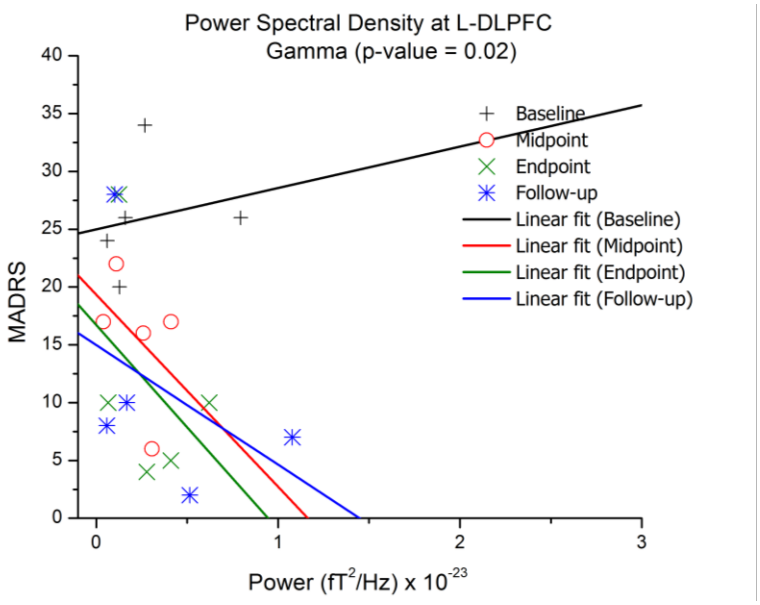

Figure 4.4: Increase gamma power at the L-DLPFC is correlated with an improvement in depressive symptoms. Linear regression models of MADRS versus PSD grouped in time for gamma band, including all subjects, show that an increase in high-frequency power is indicative of lower MADRS or better clinical outcome. Each symbol represents a different subject.

Opposite effects of functional connectivity in high and low frequency bands between L-DLPFC and remote regions

Changes in functional connectivity of L-DLPFC and several regions of interest (ROI) in the depressive circuit were observed. An increase in mean coherence in the delta band correlated with better clinical outcome for depression in the connectivity analysis between L-DLPFC and pACC ($p = 0.03$) and between L-DLPFC and amygdala ($p = 0.03$) as shown with a linear regression of MADRS versus coherence (Figure 4.5). In contrast, a decrease in mean coherence in the gamma band correlated with better clinical outcome in the connectivity analysis between L-DLPFC and sACC ($p = 0.01$). Also, this increase in coherence from baseline to endpoint in delta band was observed over the entire area of stimulation for the responders when mapped onto the cortex. Furthermore, the nodes involved in modulating connectivity were common for amygdala and sACC (Figure 4.6).

(A)

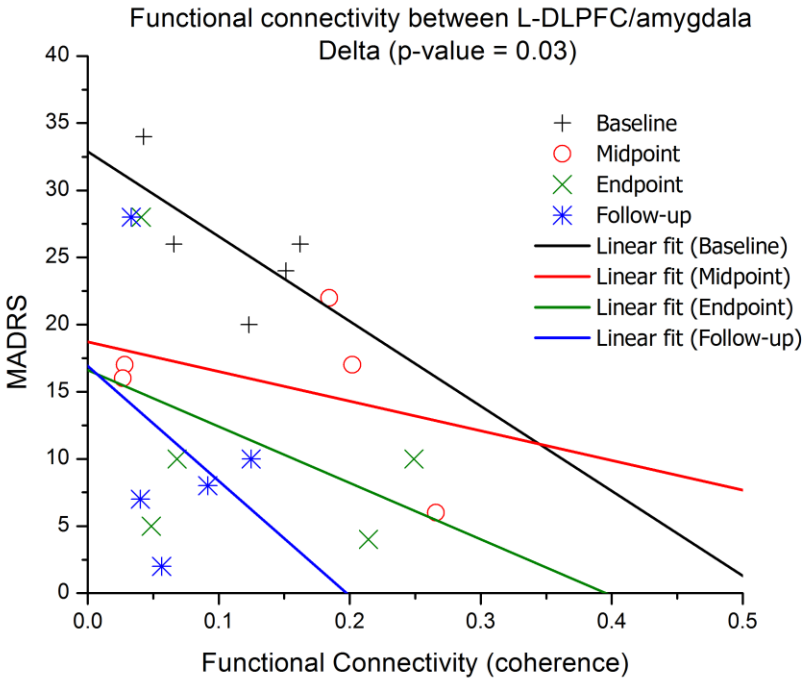
Functional connectivity between L-DLPFC/amygdala
Delta (p-value = 0.03)
MADRS
Functional Connectivity (coherence)
Baseline
Midpoint
Endpoint
Follow-up
Linear fit (Baseline)
Linear fit (Midpoint)
Linear fit (Endpoint)
Linear fit (Follow-up)

(B)

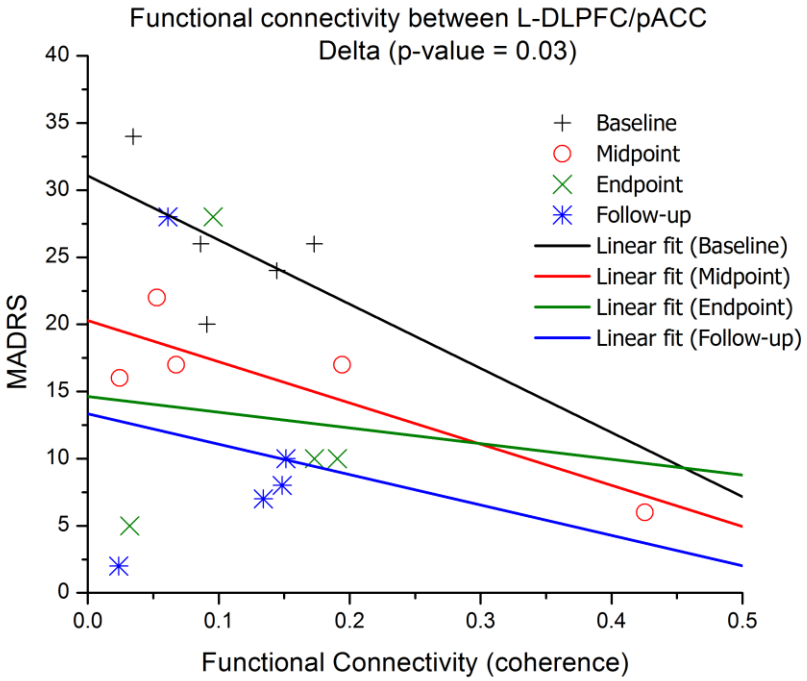
Functional connectivity between L-DLPFC/pACC
Delta (p-value = 0.03)
MADRS
Functional Connectivity (coherence)
Baseline
Midpoint
Endpoint
Follow-up
Linear fit (Baseline)
Linear fit (Midpoint)
Linear fit (Endpoint)
Linear fit (Follow-up)

(C)

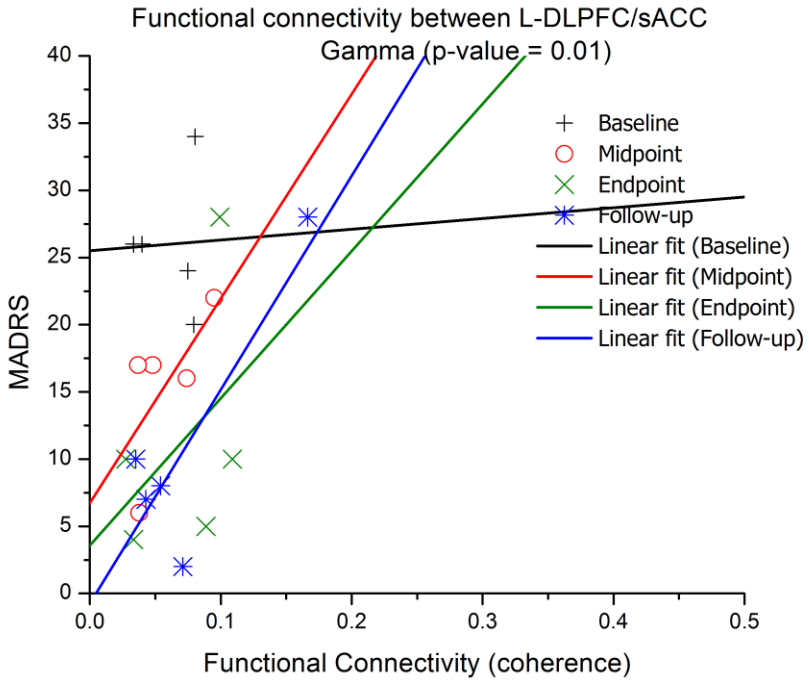

Figure 4.5: Increase in delta connectivity between L-DLPFC/pACC (A); L-DLPFC/amygdala (B); and decrease in gamma connectivity between L-DLPFC/sACC. Linear regression models of MADRS versus coherence show that there is a significant linear relationship between connectivity and an improvement in depressive symptoms.

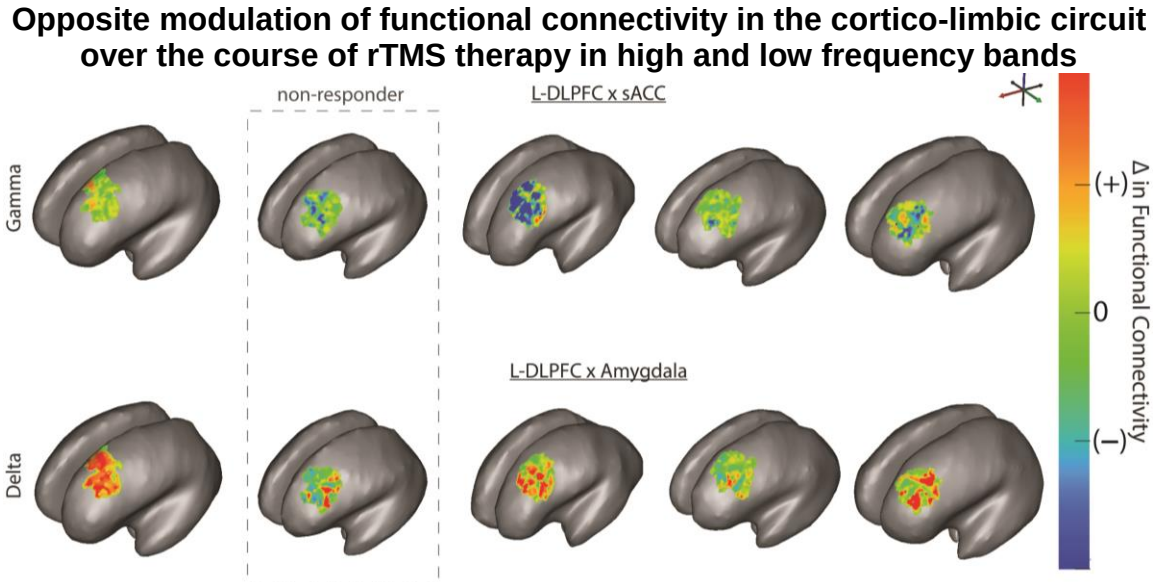

Figure 4.6: rTMS modulates connectivity over the L-DLPFC in responders. L-DLPFC/amygdala coherence in delta band (bottom) increased from baseline to endpoint over the entire area of stimulation for responders. An opposite effect was observed with a decrease in L-DLPFC/sACC coherence in gamma band (top) from baseline to endpoint over the entire area of stimulation for responders. The nodes in L-DLPFC contributing to change in connectivity are common for both amygdala and sACC for all patients.

IV. Discussion

The target of rTMS stimulation is the L-DLPFC as this region tends to show diminished function in individuals with MDD. This area is implicated in working-memory tasks, attention, and long-term memory storage and consolidation. Our results support the hypothesis that longitudinal changes are reflected in the PSD and connectivity analyses of ongoing MEG data in the resting-state.

An increase in gamma power at the L-DLPFC was correlated with an improvement in depressive symptoms. We posit that this increase may reflect a rise in metabolic activity of the DLPFC, which contributes to improvement of symptoms. Gamma oscillations have previously been linked to increased attentional processes (Benchenane et al., 2011). One mechanism of gamma modulation at a pharmacological level involves GABAergic interneurons. These cells contribute to synchronization of the pyramidal neurons in the DLPFC during tasks that require increased cognitive effort. Furthermore, GABA-mediated inhibition has shown to be sufficient in generating gamma oscillations (Barr et al., 2009).

Previous evidence also points to GABAergic involvement in antidepressant response (Bajbouj et al., 2005; Yue et al., 2009). Animal models of depression have shown that GABA agonists have antidepressant activity (Petty, 1995; Yue et al., 2009). If inhibition is facilitated by fast acting $GABA_A$ receptors, oscillation frequency will correspond to the gamma band (Buzsaki, 2006). Therefore, an increase in gamma power for responders can be attributed to GABA-mediated inhibition. Another consequence of GABA-mediated inhibition is synchronization of large neuronal populations, leading to increased long-range functional connectivity (Fingelkurts et al., 2004). Changes in

synaptic plasticity are directly related to changes measured in functional connectivity and the strength of a synapse can further dictate the effect of inhibition (Buzsaki, 2006). The depressive circuit targeted for DBS includes amygdala, pACC, sACC, and the NAc (Holtzheimer & Mayberg, 2011; Krishnan & Nestler, 2008; Ressler & Mayberg, 2007). The most effective targets for DBS are sACC and amygdala. This evidence further lends credence to our results that imply the significance of modulating connectivity between these specific regions (L-DLPFC/sACC , L-DLPFC/pACC and L-DLPFC/amygdala).

Activity in sACC contributes greatly to limbic-cortical dysregulation (Greicius et al., 2007; Mayberg, 1997). Depression severity has been shown to correlate positively with functional connectivity in sACC. In addition, increased connectivity of the default mode network in depression was also driven by this region (Greicius et al., 2007). Fox et al. also showed that the magnitude of relative disconnectivity (anticorrelation) between L-DLPFC and ACC was indicative of depression severity (Fox, Halko, et al., 2012). The distinct role of subregion functional connectivity is corroborated by differential anatomical connectivity of the pACC and sACC, suggesting a strong connection of pACC to frontal regions versus sACC to limbic regions (Johansen-Berg et al., 2008). These studies support our observed results of increased coherence with an improvement in depressive symptoms, suggesting that part of the antidepressant mechanism of rTMS may be remote suppression of the sACC, as this region has been shown to be hypermetabolic in depressed individuals.

Another noteworthy finding is that the decrease in coherence was constrained to the gamma band for sACC, whereas the increase in coherence was observed in delta band for pACC and amygdala. Different frequency bands may enable the multiplexing of

channels of communication for different functional brain networks. Communication through coherence is usually controlled by inhibitory windows (Benchenane et al., 2011). Functional connectivity in lower frequency bands has been associated with higher cognitive tasks. Previous research has also demonstrated that anatomically distributed EEG coherence increased in lower frequencies, particularly the delta band during creative thought (Gruzelier, 2009; Petsche, 1996). Furthermore, neuroimaging and neurophysiological studies have reported that long-distance integration is coordinated by lower frequencies, whereas short-distance networks are coordinated by higher frequencies (Buzsaki, 2006; Leuchter et al., 2012). In particular for mood disorders, an fMRI study (Anand et al., 2005b) showed an increase in low-frequency BOLD (Blood-oxygen-level dependent) fluctuation (LFBF) correlation between ACC and limbic regions in patients after treatment for depression. Another study (Chepenik et al., 2010) identified a negative correlation in low-frequency resting-state fMRI activity between the ventral PFC and amygdala in healthy subjects compared to those with bipolar disorder. These reports corroborate our current findings of increased connectivity in the delta band correlating with better clinical outcome.

According to an MEG study (Hillebrand et al., 2012) on resting-state functional connectivity, there is a positive correlation between patterns of source power and functional connectivity. A modeling study (Chawla 1999,2000) also showed increased phase locking between two connected neuronal populations resulting in increases in both power and functional connectivity. Based on these studies and the findings for increased gamma power in L-DLPFC that relate to increased metabolic activity in that region, we suggest that the decreased gamma connectivity with sACC is a result of decreased

gamma power at the sACC and hence lower source activity. As described earlier, decreasing metabolic activity in sACC has corresponded to an improvement in depressive symptoms for various antidepressant studies.

Lastly, the modulation in coherence between frontal and limbic regions was observed over the entire area of stimulation for responders when mean connectivity was mapped onto the L-DLPFC. This finding implies that stimulation of responders engaged functional connections that were relevant for clinical improvement and nonresponders were effectively lacking in engaging those essential connections. In a previous study investigating EpCS for depression (see Chapter 3) (Pathak et al., 2012), stimulation using the mixed mode polarity, in which the configuration of the active electrode alternated between anode and cathode in a pseudorandom manner, was effective in achieving an antidepressant response. This response was likely due to recruitment of a wider range of neurons owing to characteristic differences in anodic and cathodic stimulations (Pathak et al., 2012; Wongsarnpigoon & Grill, 2008). Another study (Riva-Posse et al., 2014) investigating fiber tracts concluded that the involvement of bilateral forceps minor, cingulate bundle, and short descending midline fibers was predictive of clinical response. Riva-Posse et al. emphasized that the anatomical location of active electrodes was not the source of variability, but instead it was the hub location where these three fibers intersected that determined potential of response.

V. Conclusion

There are a few limitations that should be addressed in future studies as the field advances. First, interaction of TMS with prescribed medication is not clearly understood.

There is a possibility that changes in medication can affect cortical excitability which might necessitate a re-evaluation of the TMS "dose". Additionally, we analyzed data from a small sample size. However, our findings are robust for all patients and the results are selective for specific targets. A comparison of PSD in the right occipital cortex as a control region did not result in a linear trend similar to the one observed at the L-DLPFC. The primary finding from this study is that in addition to local changes, high-frequency rTMS modulates several nodes of the depressive circuit during an effective clinical response. We postulate that this approach could provide valuable insights about patients evaluated for DBS surgery by advising physicians about which regions and functional connections to focus on for a robust response.

CHAPTER 5: HOW DOES STIMULATION OF DIFFERENT TARGETS IN THE DEPRESSIVE CIRCUIT AFFECT ANTIDEPRESSIVE RESPONSE?

I. Introduction

MDD is a highly disabling condition that affects a sixth of the American population (Kessler et al., 2005; Krishnan & Nestler, 2008). Because of its heterogeneity, many patients are resistant to commonly prescribed therapies. In recent years, neuromodulation therapies such as deep brain stimulation (DBS), chronic epidural stimulation (EpCS), and repetitive transcranial magnetic stimulation (rTMS) have found some success with treating this population. However, there are differing theories regarding the etiology of depression that have led to an investigation of several targets for neuromodulation therapy with variable efficacies. In particular for DBS, studies have focused on the sACC, ventral capsule/ventral striatum (VC/VS), medial forebrain bundle, and NAc (Bewernick et al., 2010, 2012; Coenen et al., 2010; Holtzheimer et al., 2012; Malone et al., 2009; Mayberg et al., 2005; Schlaepfer et al., 2013).

Effects of differences within a target have been evaluated previously for Parkinson's disease (Nestor et al., 2014). In the Nestor et al. study, the hypothesis was that stimulation to specific subregions or neighboring fiber bundles would engage remote areas and result in better motor outcomes. Similarly, there is increasing evidence to approach MDD as a circuit-level disorder. A recent study demonstrated that clinical response was predicted by stimulation of specific white matter pathways and not just the anatomical location of active electrodes (Riva-Posse et al., 2014). The motivation for this study was to assess variability within a site of stimulation to better understand clinical improvement due to DBS for depression.

We studied a rodent model to answer the question, can variability in electrode placement account for behavioral differences in an antidepressive-like response? Animal models are valuable in providing insights about in vivo effects of DBS while allowing for a controlled environment (Cohen et al., 1998; Hamani, Diwan, Macedo, et al., 2010; Lim & Helpern, 2002). We investigated DBS at the ventromedial prefrontal cortex (VMPFC), white matter fibers of the frontal region (WMF), and NAc to evaluate the effects of stimulation location within these target regions.

As these three structures are interconnected to some degree, an initial hypothesis was that by stimulating them, we would be modulating the same circuit at different levels. However, Hamani et al. have recently shown that, despite similar antidepressive-like responses, DBS at these regions induces specific patterns of metabolic activity and functional connectivity, as measured by *zif268* expression (Hamani et al., 2014).

One of the most commonly used and validated preclinical screeners for the effectiveness of antidepressant medications or neuromodulation techniques is the forced swim test (FST) (Hamani & Temel, 2012). The degree of behavioral response varies between individuals regardless of the treatment. In this chapter, we investigated whether small variations in electrode placement within the VMPFC, WMF, and NAc can account for notable differences in behavioral outcomes in rats given DBS during the FST. We hypothesized that improvement in behavior is spatially dependent on stimulation location within a target.

II. Methods

Male Sprague-Dawley rats (250-300 g) were anesthetized with halothane and electrodes were implanted in one of the following targets (Paxinos and Watson, 1998): 1) VMPFC; anteroposterior (AP) + 3.0 mm, lateral (L) ± 0.4 mm, and depth (D) 5.6 mm; 2) WMF (forceps minor) AP +2.7 mm, L 1.4 mm, D 5.6 mm; 3) NAc AP +1.6 mm, L 1.2 mm, D 8.0 mm. Monopolar stainless steel electrodes (250 μm in diameter and 0.5 mm of exposed surface) were used as cathodes. An epidural screw placed over the somatosensory cortex was used as the anode (AP 0.5, L ± 1.5, D 1.0 mm) (Paxinos and Watson, 1998). Controls had holes drilled into the skull but were not implanted with electrodes. The VMPFC target has been considered homologous to the human sACC. The WMF target was chosen because it is the largest frontal brain structure containing both commissural and projection fibers. This target is not a homolog of the anterior limb of the internal capsule (ALIC), but it is partially composed of cortical projections that innervate the thalamus, basal ganglia, and brainstem nuclei.

The FST was conducted one week after electrode implantation. On testing day one, rats were individually placed in a cylinder filled with 25 ± 1°C water for 15 minutes (Detke and Lucki, 1996; Detke et al., 1995). Thereafter, DBS-treated animals received continuous stimulation for four hours (ANS model 3510) at 100μA, 130Hz, and 90μsec (Hamani, Diwan, Isabella, et al., 2010). On the following day, rats in the DBS groups received two hours of stimulation followed by a five-minute swimming session during which the predominant behavior (immobility, swimming, or climbing) of the animals was scored at five-second intervals (Detke and Lucki, 1996; Detke et al., 1995).

Animals were sacrificed an hour after behavioral testing by decapitation following ketamine/xylazine anesthesia. We used *in situ* hybridization using ^{35}S-UTP labeled riboprobes to measure *zif268* (Hamani et al., 2014a; Creed et al., 2012). After hybridization, slides were exposed to Kodak BioMax film for 6 days at 4°C with calibrated radioactivity standards. Film analyses were conducted with an MCID system (Interfocus, UK).

We conducted a probabilistic analysis (Figure 5.1) using MATLAB (Mathworks Inc, Natick, MA) to evaluate within-target effects of stimulation. The coordinates of electrode implants for all animals were determined from histology and mapped onto the Paxinos atlas. Electrode locations from the right hemisphere were mirrored onto the left hemisphere for this analysis as confirmed by histology. One immobility score was assigned per rat, which corresponded to both left and right electrodes in that particular animal. Next, a volume of tissue activation (VTA) was computed based on a multi-compartment model of excitable neuronal elements around each electrode location using stimulation parameters. A binary mask was created to label voxels within the sum of VTAs for a particular target. Each voxel was then assigned an average immobility score based on the results of the FST from every rat. Only voxels contained within two or more VTAs were included in the average analysis. The mapped scores (average immobility per voxel) were visualized in SCIRun (Center for Integrative Biomedical Computing, University of Utah) to further explore the effects of DBS within a particular target.

We further explored the data by examining the distribution for each target. If the distribution of the data or its residuals was normal, a generalized linear regression (Eq 11) model was used to determine the significance and magnitude of the effect of location

in each axis (M-L, D-V, A-P). All statistical analysis was done in MATLAB (Mathworks Inc, Natick, MA).

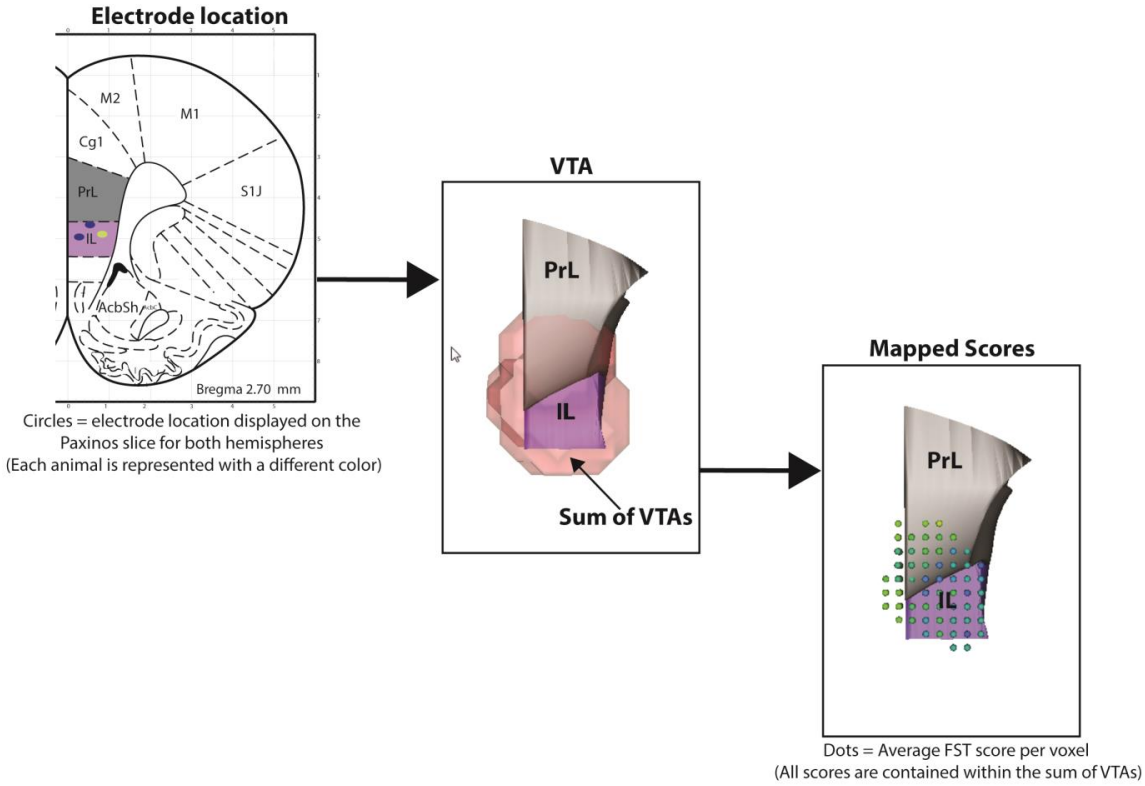

Figure 5.1: Probabilistic analysis of improvement with DBS for depression. Stimulation locations for all animals in both hemispheres were mapped on the Paxinos atlas. Subsequently, a volume of tissue activated (VTA) was computed to determine the extent of stimulation. Lastly, behavioral scores from the FST were mapped onto VTA voxels for spatial analysis.

III. Results

Antidepressive response was related to stimulation in the anterior region of VMPFC

Data from 29 male Sprague-Dawley rats were analyzed in this study. Eleven rats (22 hemispheres) were bilaterally implanted in the VMPFC. Stimulation was constrained in the A-P axis from Bregma 2.20 mm to Bregma 3.70 mm. Average immobility scores per voxel ranged from 54.9 to 89.3 and were normally distributed (Figure 5.2A). A linear regression model indicated a significant effect of location in all axes with the highest

magnitude in the D-V and A-P axes (Table 5.1, Figure 5.3A). Higher immobility scores were correlated with stimulation in the dorsal/posterior region versus the anterior regions of the VMPFC (Figure 5.4). Also, voxels that represent the highest immobility were in the vicinity of the infralimbic cortex (IL)/ prelimbic cortex (PrL) border.

Spatial dependence of stimulation at the VMPFC			
Variable	Coefficient (β)	Std. error	p-value
intercept	128.91	3.26	< 0.01
x (M-L)	2.06	0.73	< 0.01
y (D-V)	9.49	0.59	< 0.01
z (A-P)	-6.20	0.41	< 0.01

Table 5.1: Regression table for general linear model of stimulation in the VMPFC

Antidepressive response was related to stimulation in the lateral region of NAc

Eight rats (16 hemispheres) were bilaterally implanted in the NAc. All stimulation was constrained to the accumbens core (Bregma 1.20 mm- Bregma 1.70 mm). Compared to other targets, NAc displayed a better antidepressive response. Overall, the range of average immobility per voxel for stimulation in the NAc was 47.3 to 79.5 with a segregated distribution, but normal distribution of residuals (Figure 2B). For the NAc, a linear regression fit indicated a significant effect in the M-L and A-P with high magnitude (Table 5.2, Figure 5.3B). Higher immobility was correlated with stimulation in the lateral/posterior region versus medial region of the activated surface (Figure 5.5).

Spatial dependence of stimulation at the NAc			
Variable	Coefficient (β)	Std. error	p-value
intercept	34.86	36.11	0.33
x (M-L)	24.29	1.98	< 0.01
y (D-V)	0.60	5.36	0.91
z (A-P)	-10.45	2.54	< 0.01

Table 5.2: Regression table for linear regression of stimulation in the NAc

Antidepressive response was related to stimulation in the dorsal region of WMF

Ten rats (20 hemispheres) were bilaterally implanted at the WMF of the frontal regions ranging from Bregma 2.2 mm to Bregma 2.7 mm in the A-P axis. Average immobility per voxel ranged from 67.9 to 91.7 with a segregated distribution, but normal distribution of residuals (Figure 2C). The response due to stimulation was significant in the D-V axis around y = 4.8 mm (distance from the horizontal plane passing through Bregma and Lambda on the surface of the skull) with a high magnitude of effect (Table 5.3, Figure 5.3C). The trend indicates higher immobility in the ventral region versus dorsal region of the activated surface of WMF (Figure 5.6).

Spatial dependence of stimulation at the WMF			
Variable	Coefficient (β)	Std. error	p-value
intercept	-3.02	2.54	0.23
x (M-L)	1.86	1.02	0.06
y (D-V)	-13.85	0.62	< 0.01
z (A-P)	4.92	0.98	< 0.01

Table 5.3: Regression table for linear regression model of stimulation in the WMF

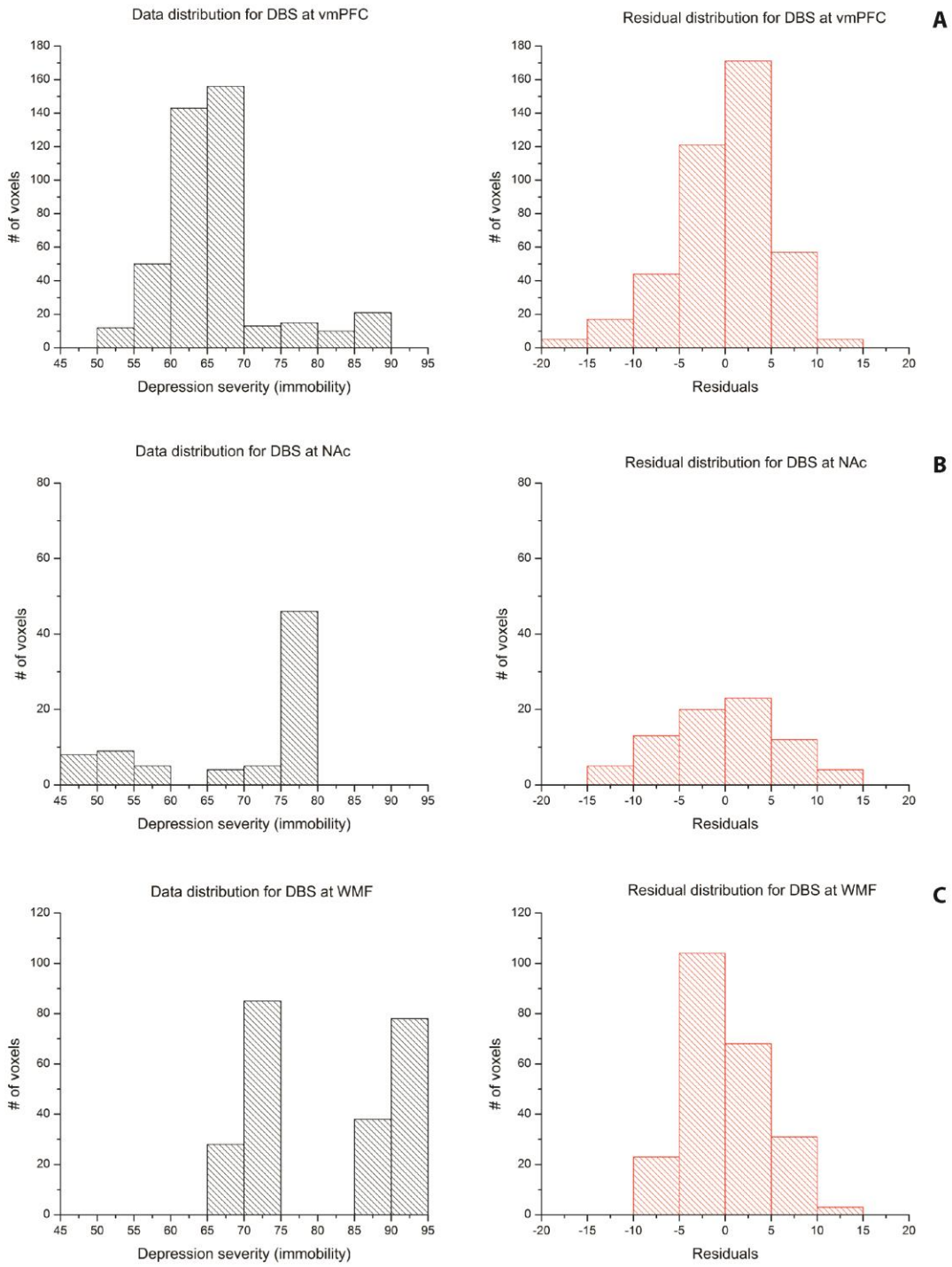

Figure 5.2: Distribution of depression scores at each target (left) and respective residuals (right). VMPFC (A); NAc (B); WMF (C)

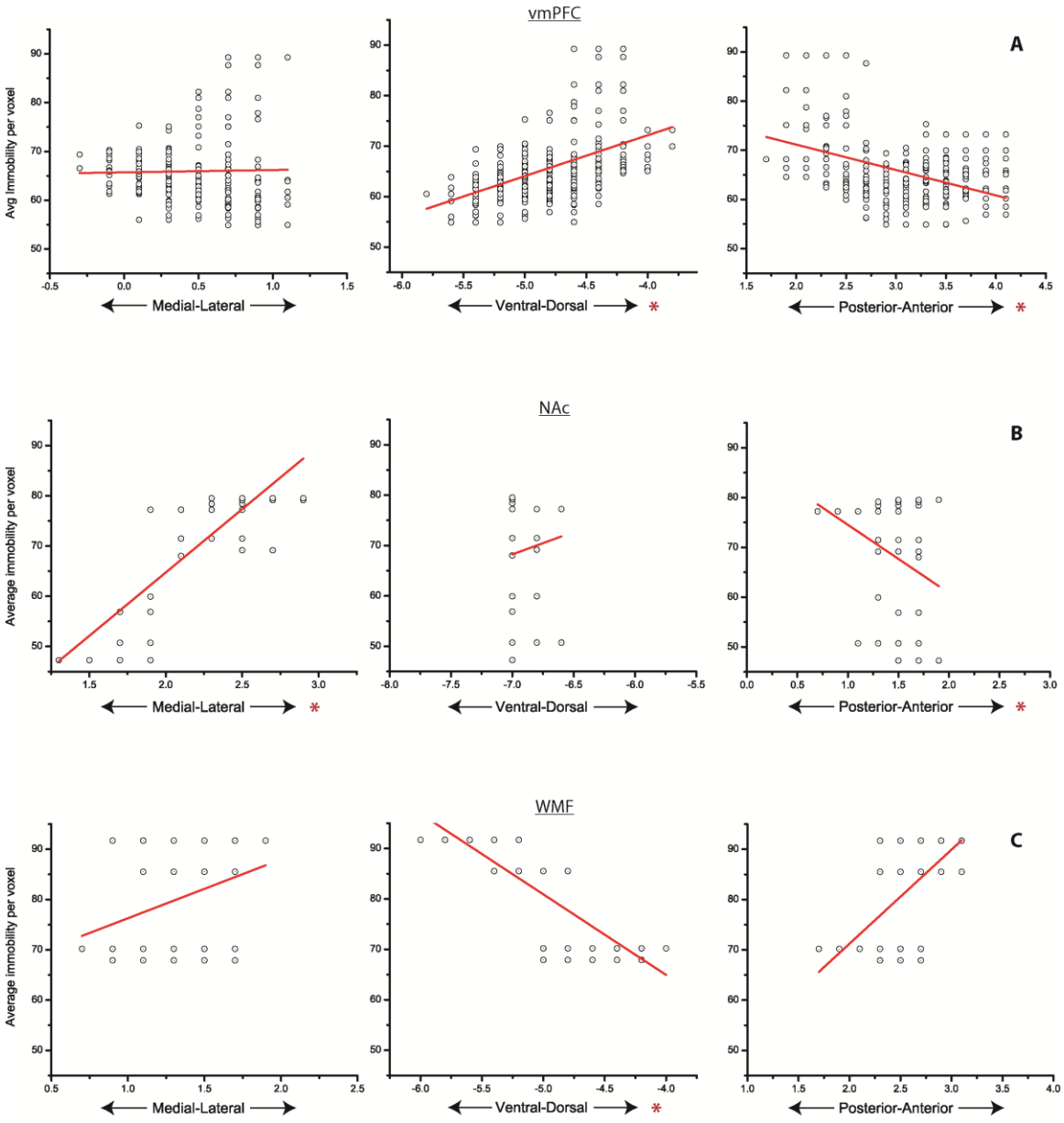

Figure 5.3: Scatter plots and a line of fit (red) showing the relationship between average behavioral outcomes and the location of a stimulated voxel along a particular axis: M-L (left), D-V(middle), A-P (right). Results are shown for vmPFC (A), NAc (B), and WMF (C).

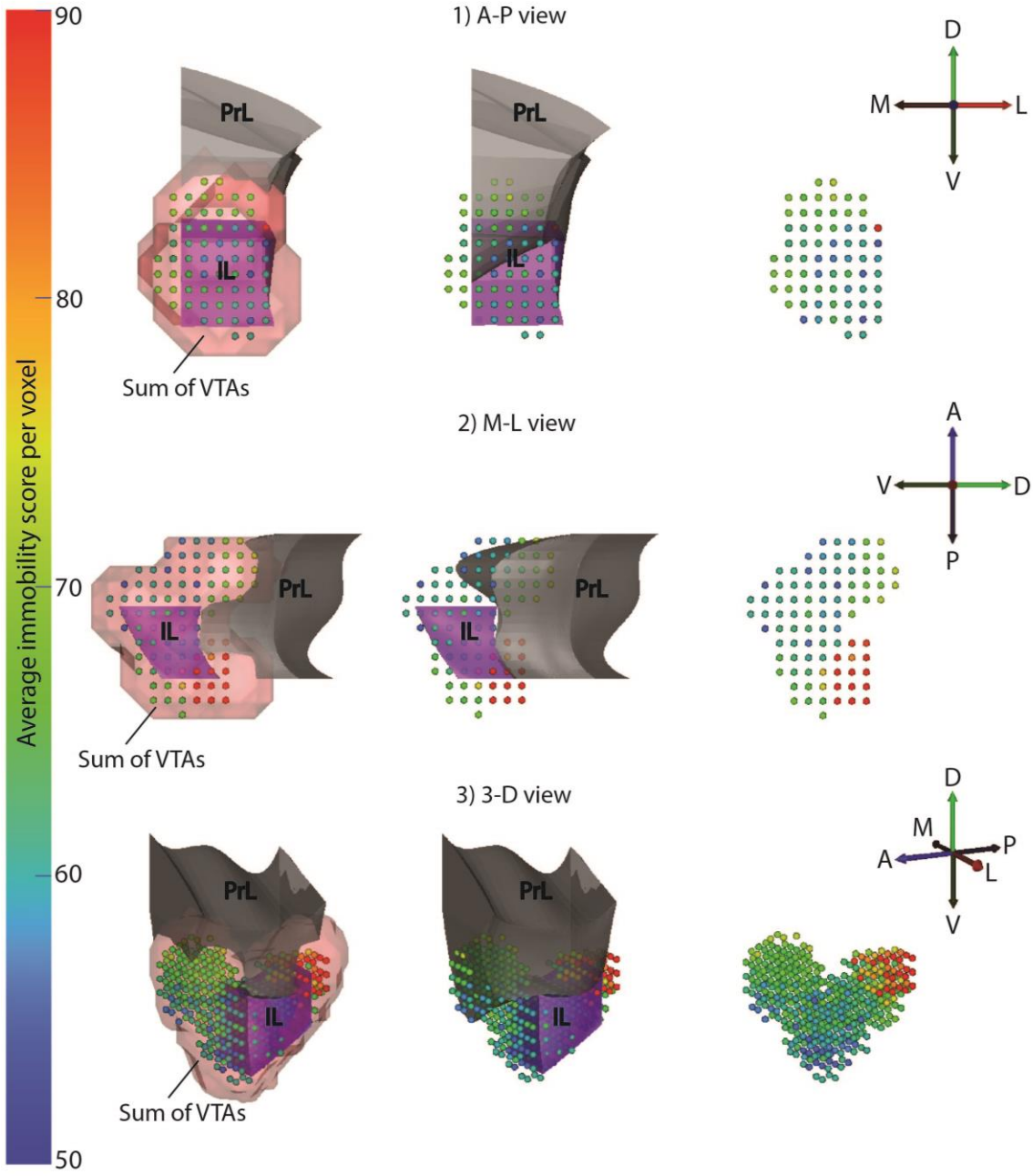

Figure 5.4: Surfaces: IL (purple), PrL (gray), sum of all activated regions in all animals (pink).
According to this figure, there is a strong trend that indicates high immobility (and therefore high depression) in the dorsal/posterior region versus low immobility in the anterior region of the activated surface in the VMPFC.
Axes: +blue = anterior; +red = lateral; +green = dorsal

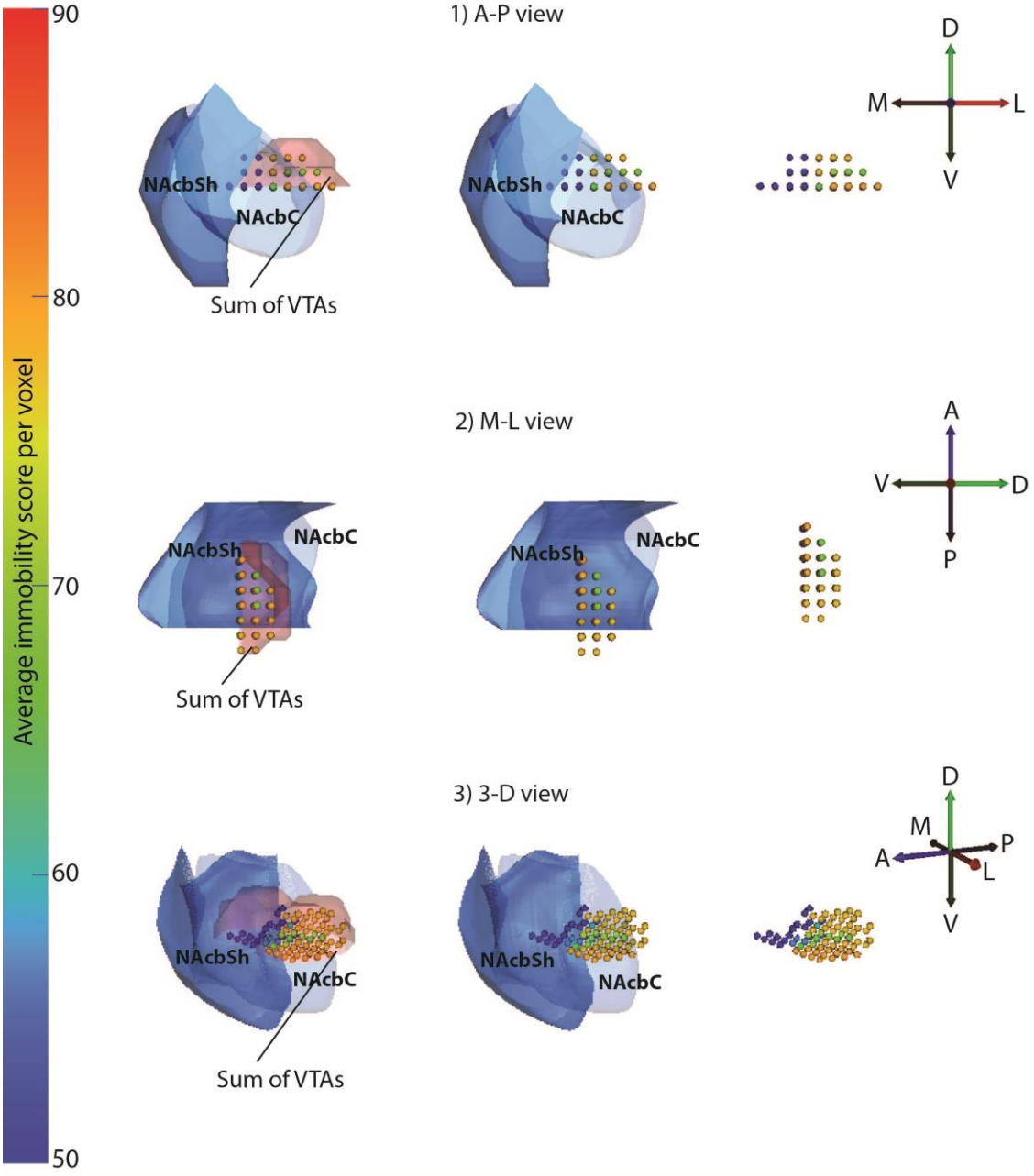

Figure 5.5: Surfaces: NAc core (light blue) and shell (dark blue), sum of all activated regions in all animals (pink).
According to this figure, there is a strong trend that indicates high immobility (and therefore high depression) in the lateral region versus low immobility in the medial region of the activated surface in the NAc
Axes: +blue = anterior; +red = lateral; +green = dorsal

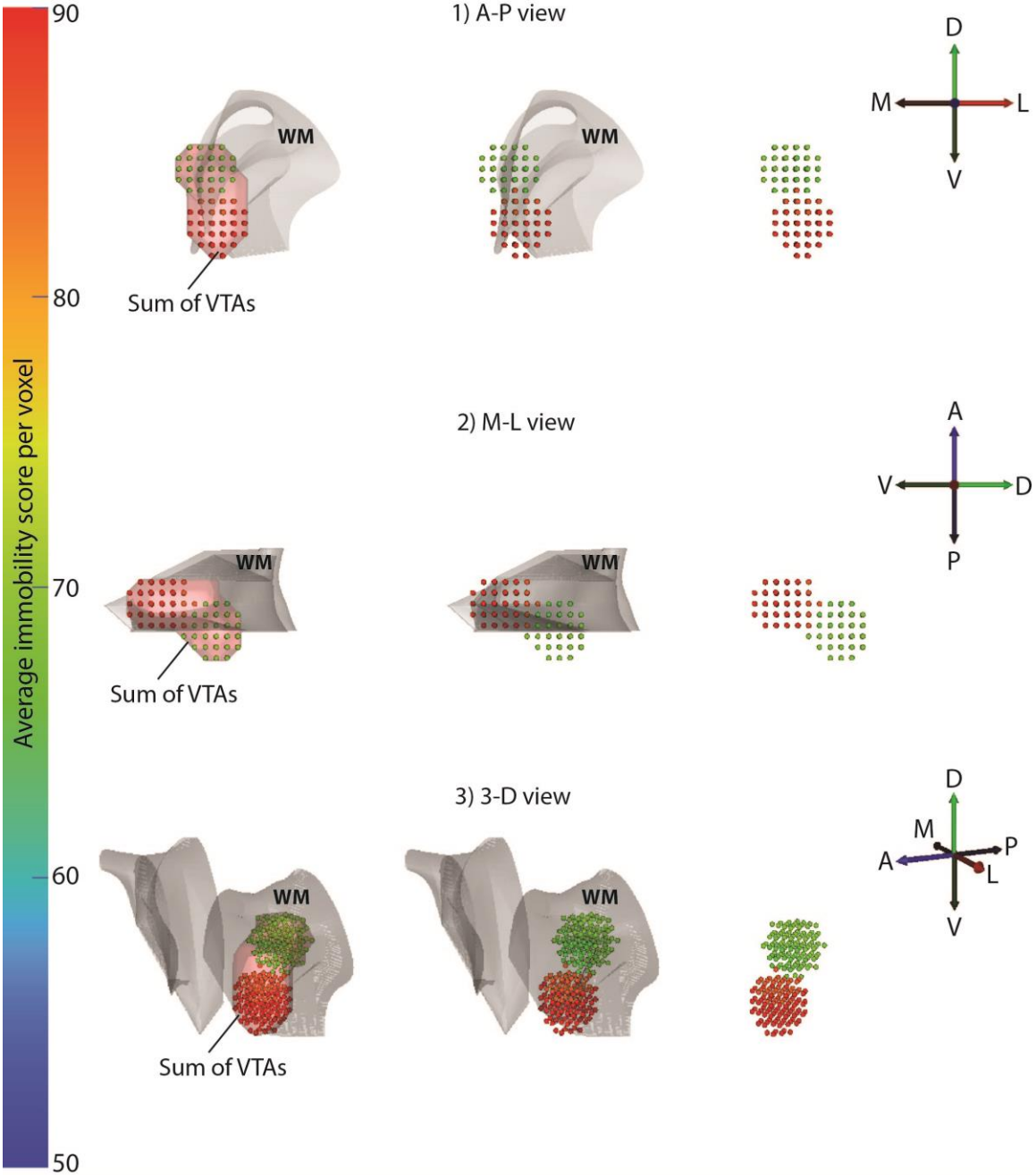

Figure 5.6: Surfaces: White matter ranging from 2.2 mm - 2.7 mm in the A-P axis on Paxinos (light-gray), sum of all activated regions in all animals (pink).
According to this figure, there is a strong trend that indicates high immobility (and therefore high depression) in the ventral region versus low immobility in the dorsal region in the activated WMF
Axes: +blue = anterior; +red = lateral; +green = dorsal

IV. Discussion

Neuron response to DBS is highly dependent on location of electrode, stimulation parameters, and synaptic influences (McIntyre et al., 2004). The goal of our study was to evaluate the effect of stimulation location in three targets using DBS for depression in a rodent model. Our hypothesis was that improvement in depression as measured by reduction in immobility depends on the target and the position of the active electrode within a target.

Several studies use neuroimaging and computational models to explore the effect of electrode location within a stimulation target on behavioral outcomes. However, to our knowledge, this is the first time probabilistic analysis has been applied to animal models. Our previous study investigating the role of stimulation parameters in EpCS concluded that an anterior/lateral placement of electrodes within the L-DLPFC contributed to higher improvement (Pathak et al., 2012). In a model (McIntyre et al., 2004) examining the cellular effects of DBS, McIntyre et al. showed that neuron response was contingent on the position and orientation of the axon relative to the electrode. The initial hypothesis regarding DBS was that it served as a "reversible lesion" (Benabid et al., 1991; Benazzouz et al., 1995; Holtzheimer & Mayberg, 2011), but evolving research points toward a more complex mechanism including both excitation and inhibition of neuronal elements (cell bodies and axons) within the field of stimulation (Holtzheimer & Mayberg, 2011; Iremonger et al., 2006; McIntyre et al., 2004). Observed results from the current study further this notion of complexity by demonstrating the significance of within-target stimulation, which is likely inducing response by activating a complex pattern of neuronal elements.

Specifically, we advanced previous findings by evaluating the role of stimulating individual voxels in contributing to an antidepressive-like response in DBS. We investigated the VMPFC, which is equivalent to the human sACC, WMF of the frontal regions, and the NAc (Gabbott et al., 2003; Hamani et al., 2014; Hamani, Diwan, Macedo, et al., 2010; Takagishi & Chiba, 1991).

VMPFC is pivotal in the pathophysiology of rodent depression. The VMPFC→dorsal raphe nucleus (DRN) pathway was deemed key in inducing an antidepressive response (Artigas, 2014; Warden et al., 2012). Furthermore, repeated DBS at the target increased excitatory inputs to 5HT neurons and reversed neuroplastic changes that formed during the development of a depressed phenotype (Veerakumar et al., 2013). In the VMPFC, we found that an antidepressive response was related to stimulation in the ventral/anterior region. Because the rodent VMPFC has a multitude of projections to distinct cortical and subcortical sites, the stimulation location will have a specific effect on response (Artigas, 2014). Location in the D-V axis had the greatest influence on behavioral response. Both IL and the PrL nuclei are separated along this axis. Earlier studies have shown distinct amygdalar and insular projections to these nuclei (Hoover & Vertes, 2007; McDonald et al., 1996; Vertes, 2004). The efferents from these VMPFC nuclei are distinctive as well and consistent with their respective functions (McDonald et al., 1996; Vertes, 2004). IL is typically regarded as the visceromotor center and is involved with the inhibition of subcortical structures during emotional processing. It projects widely to the amygdala, including superficial nuclei, basolateral nuclei, and the central nucleus. In contrast, the PrL participates primarily in cognitive processes with virtually no projections to the superficial nuclei of the amygdala (Hoover & Vertes,

2007). One study characterizing emotional conflict showed that the dorsal and ventral regions of the ACC and medial PFC are functionally different (Etkin et al., 2011) Both dorsal ACC and mPFC are involved in appraisal and experience of emotional memories, whereas the ventral ACC and mPFC contribute to inhibition and regulation by mediating between dorsal areas and amygdala since there are no direct connections between these regions.

sACC, the human correlate to rodent VMPFC, has also shown reciprocal connections with the amygdala (Johansen-Berg et al., 2008). Additionally, a clinical DBS trial (Riva-Posse et al., 2014) showed the functional variability of sACC. In order to achieve clinical response, specific white matter tracts (forceps minor, cingulum bundles, uncinate fasciculus) needed to be recruited. These fiber tracts connect remote areas of the brain with the sACC and modulate the depressive circuit as a whole. One of those regions is the NAc, which connects to the sACC through the medial branch of the uncinate fasciculus.

The NAc plays a central role in reward circuitry. It is investigated as a DBS target because of the prominent anhedonic symptoms in depression. According to a previous clinical study, DBS at NAc decreased metabolism in sACC and amygdala, both of which are hypermetabolic in depression. In addition, an antianhedonic effect was observed in responders (Bewernick et al., 2010). However, in a recent rTMS study, stimulating at the L-DLPFC did not result in altered connectivity with NAc, implying that although it may alleviate symptoms, its role in reversing MDD is not principal (see Chapter 4). In our analysis, the antidepressive response was related to stimulation in the medial region of NAc. A study (Usuda et al., 1998) using biotinylated dextran amine anterograde tracer

demonstrated the differential connectivity patterns of the dorso-medial and ventro-lateral regions of the NAc core. Although both regions project to nodes of the reward circuit, particularly the ventral pallidum, targets of the dorso-medial region also include substantia nigra reticulata and the lateral hypothalamus whereas those of the ventro-lateral region include globus pallidus and substantia nigra compacta. These efferents imply that dorso-medial NAc contributes to motor regulation and ventro-lateral NAc supplements motivational processes. Our results exhibit this characteristic in the M-L axis. Stimulation in the medial region of the core correlated with low immobility/high improvement in behavioral response.

Stimulation in this target also corresponded to the best antidepressive response when compared to the other DBS targets. One reason for that could be the task (FST) used to assess antidepression in rodents is more sensitive to physical behavior than mood. Anhedonia is defined as the lack of desire to participate in an activity and DBS at this region is effectively reversing this symptom as measured with a decrease in immobility. The results from analyzing this site in the context of previous findings suggest consideration of MDD as a heterogeneous disorder for which it might be more beneficial to customize treatment targeted toward a specific symptom instead of a one-size-fits-all approach.

The role of fiber tracts in modulating the depressive circuit has been established (Gutman et al., 2009; Li et al., 2007; Riva-Posse et al., 2014). However, white matter connectivity has been shown to be rather complex. A tractography study examining the projections of ALIC found that the pattern of connectivity was spatially dependent in a multifarious manner with afferents and efferents of the thalamus (Gutman et al., 2009).

Rats lack a developed ALIC, and therefore the largest white matter structure, forceps minor, was chosen. Also, this white matter structure contains commissural and projection fibers (Hamani & Nóbrega, 2010; Hamani et al., 2014). The response at this site was quite segregated in the D-V axis with antidepressive-like behavior correlating to stimulation in the dorsal region, possibly because these fibers have specific projections and the response is a result of modulating nodes at the end of them. Fibers passing dorsally are likely connecting regions that are more significantly involved in the pathology of depression.

These results lead to two plausible theories: 1) the activated sub-region activity within a target is responsible for improved behavioral response or 2) the activated sub-region projects differentially to nodes of the depressive circuit responsible for behavioral improvement. The latter theory has become increasingly relevant as neuroimaging studies provide evidence for changes in connectivity and synaptic plasticity and mandate we redefine neurological conditions as network-level disorders. Observations from this study offer a possible factor in characterizing the variability of response in an extremely heterogeneous condition.

Nevertheless, there are some limitations to this study. First of all, we are investigating an animal model, which is a great physiological analog, but does not quite allow the assessment of mood. Also, these animals were implanted bilaterally, but laterality was not taken into account during the analysis. Since there was only one immobility score per animal, it was difficult to discern how each hemisphere contributed to the outcome. In addition, all electrode locations were mapped onto the Paxinos atlas, disregarding the inherent neuroanatomical variability between subjects.

V. Conclusion

Despite the limitations, the results of this study add value to current research surrounding DBS for depression. First, this study facilitates understanding of each individual target and sets the foundation for future studies to investigate the effect of stimulation at a particular target to improve a specific symptom. Second, it highlights the heterogeneity of each brain region and further emphasizes the significance of location in predicting the antidepressive outcome. Overall, these findings can form the foundation for future studies that should incorporate details of anatomical and functional connectivity to validate the subregion differences and optimize DBS therapy for MDD.

CHAPTER 6: CLINICAL IMPACT

Practical application of our research in clinical practice is the ultimate motivation for biomedical engineers to delve into the complexity of neuromodulation therapies. Ideally, physicians would prefer an in-office device that could help diagnose, navigate, and noninvasively stimulate the brain to treat MDD. Such a device can be implemented in a few years with integrative studies and incorporation of advanced technologies, but a more immediate and tangible problem faces the clinical community.

Currently, there are no clinically acceptable methods to predict treatment response. The methods described in this dissertation are certainly a step in that direction. First of all, the results indicate that functional neuroimaging can be used as an indirect biomarker of response. Additionally, the correlative analysis of stimulation parameters, neuroimaging outcomes, and behavioral scores is a bridge to link the physiological basis of MDD to behavioral relevance.

CHAPTER 7: CONCLUSIONS AND FUTURE DIRECTIONS

MDD is a circuit-based disorder and neuromodulation therapies should be designed to interrogate the whole circuit. The findings of this dissertation are a trend in improving the predictive power of future studies in neuromodulation by combining neuroimaging with computational tools. We have shown that there are several successful ways to modulate the depressive circuit; each modality has a specific set of parameters that will help achieve a robust clinical response. It is apparent that neuromodulation effects are location dependent. However, these findings encourage us to expand our definition of location from mere anatomical coordinates to essential functional pathways. Both studies targeting the L-DLPFC showed that a wide range of neural elements needed to be recruited in order to observe a clinical response. Subregions of individual targets also present differential outcomes to stimulation. Additionally, we demonstrated that MDD patients can be broadly characterized as slow or fast responders and the type of neuromodulation prescribed should take into account an individual's unique time-constant for improvement. DBS for depression is popular, but its invasive nature makes the stakes quite high. We have established that rTMS can be used to interrogate and manipulate the circuit implicated in DBS therapy.

Future studies need to account for variables that were not explored in this dissertation. First, the durability of response should be studied beyond 2 weeks for rTMS therapy. A cost-benefit analysis of noninvasive short-term therapy versus invasive chronic stimulation can further help determine if rTMS should be used as a tool for surgical planning or as a therapeutic option. Also, anatomical connectivity can validate

interpretations of the functional connectivity analysis and the differential behavior of DBS at several targets. Lastly, this study explored only the longitudinal effects of neuromodulation. A deeper understanding of the mechanisms of action for neuromodulation can be possible only by also investigating the acute effects of stimulation with simultaneous EEG and rTMS.

APPENDIX

Transcranial Magnetic Stimulation

Bio-Savart Law (Eq 1)

$$\mathbf{B} = \frac{\boldsymbol{\mu_0}}{\mathbf{4\pi}} \mathbf{I} \int \frac{\mathbf{dl} \times \hat{\mathbf{r}}}{\mathbf{r^2}}$$

Maxwell-Faraday (Eq 2)

$$\boldsymbol{\nabla} \times \mathbf{E} = -\frac{\boldsymbol{\partial \mathbf{B}}}{\boldsymbol{\partial \mathbf{t}}}$$

Source Imaging

Linear inverse operator (Eq 3)

$$\hat{j}(t) = Mx(t) \rightarrow current\ amplitude\ at\ time\ t$$
$$M = R'G^T(GR'^{G^T} + C)^{-1}$$

M = strengths of sources
G = relates source strength to measured signal
C = data noise covariance matrix
R' = source covariance matrix

Whitening (Eq 4)

$$\widetilde{M} = R\tilde{G}^T\left(\tilde{G}R\tilde{G}^T + I\right)^{-1}$$
$$\tilde{G} = C^{-\frac{1}{2}}G \rightarrow spatially\ whitened\ gain\ matrix$$
$$C^{-\frac{1}{2}} = U_c\ \Lambda_C^2 \mathrm{U}_C^T \rightarrow eigenvalue\ decomposition$$

Computation of Solution (Eq 5)

$$A = \tilde{G}^{\frac{1}{2}} = U\Lambda V^T$$
$$\widetilde{M} = R^{1/2}V\Gamma U^T$$
$$w(t) = U^T C^{-\frac{1}{2}} x(t)$$
$$\hat{j}(t) = R^C V\Gamma w(t) \rightarrow expected\ current$$

Depth weighting (Eq 6)

$$f_p = (g_{1p}^T g_{1p} + g_{2p}^T g_{2p} + g_{3p}^T g_{3p})^{-\gamma}$$

$$g \rightarrow columns\ of\ G$$
$$p \rightarrow source\ locations$$
$$\gamma \rightarrow order\ of\ depth\ weighting$$

Welch Algorithm (PSD)

Signal is split into overlapping segments and a periodogram is computed using discrete fourier transform (DFT)

$$f(v) = \mathcal{F}_t[f(t)](v) = \int_{-\infty}^{\infty} f(t)e^{-2\pi ivt}dt \rightarrow continuous\ fourier\ transform \quad \textbf{(Eq 7)}$$

$$F_n = \sum_{k=0}^{N-1} f_k e^{-2\pi ink/N} \rightarrow DFT \quad \textbf{(Eq 8)}$$

Coherence (Functional Connectivity)

$$C_{xy} = \frac{|G_{xy}|^2}{G_{xx}G_{yy}} \quad \textbf{(Eq 9)}$$

$$G_{xy} \rightarrow crossspectral\ density$$

$$G_{xx} and\ G_{yy} \rightarrow autospectral\ density$$

Normalized Difference

$$\Delta(m) = \frac{Timepoint(m) - Baseline(m)}{Baseline(m)} \quad \textbf{(Eq 10)}$$

$$m \rightarrow measure(PSD\ or\ coherence)$$

Generalized Linear Model

$$y = \beta_0 + \beta_1(x) + \beta_2(y) + \beta_3(z) \quad \textbf{(Eq 11)}$$

BIBLIOGRAPHY

Amaral, D. G., & Price, J. L. (1984). Amygdalo-cortical projections in the monkey (Macaca fascicularis). *Journal of Comparative Neurology*, *230*(4), 465–496.

Anand, A., Li, Y., Wang, Y., Wu, J., Gao, S., Bukhari, L., … Lowe, M. J. (2005a). Activity and connectivity of brain mood regulating circuit in depression: a functional magnetic resonance study. *Biological Psychiatry*, *57*(10), 1079–88. doi:10.1016/j.biopsych.2005.02.021

Anand, A., Li, Y., Wang, Y., Wu, J., Gao, S., Bukhari, L., … Lowe, M. J. (2005b). Antidepressant effect on connectivity of the mood-regulating circuit: an FMRI study. *Neuropsychopharmacology : Official Publication of the American College of Neuropsychopharmacology*, *30*(7), 1334–44. doi:10.1038/sj.npp.1300725

Artigas, F. (2014). Deep brain stimulation in major depression: plastic changes of 5-hydroxytryptamine neurons. *Biological Psychiatry*, *76*(3), 174–5. doi:10.1016/j.biopsych.2014.05.008

Baillet, S., Mosher, J. C., & Leahy, R. M. (2001). Electromagnetic Brain Mapping. *IEEE Signal Processing Magazine*, (November), 14–30.

Bajbouj, M., Brakemeier, E.-L., Schubert, F., Lang, U. E., Neu, P., Schindowski, C., & Danker-Hopfe, H. (2005). Repetitive transcranial magnetic stimulation of the dorsolateral prefrontal cortex and cortical excitability in patients with major depressive disorder. *Experimental Neurology*, *196*(2), 332–8. doi:10.1016/j.expneurol.2005.08.008

Banks, S. J., Eddy, K. T., Angstadt, M., Nathan, P. J., & Phan, K. L. (2007). Amygdala-frontal connectivity during emotion regulation. *Social Cognitive and Affective Neuroscience*, *2*(4), 303–12. doi:10.1093/scan/nsm029

Barker, A. T., Jalinous, R., & Freeston, I. L. (1985). NON-INVASIVE MAGNETIC STIMULATION OF HUMAN MOTOR CORTEX. *The Lancet*, *325*(8437), 1106–1107. doi:10.1016/S0140-6736(85)92413-4

Barr, M. S., Farzan, F., Rusjan, P. M., Chen, R., Fitzgerald, P. B., & Daskalakis, Z. J. (2009). Potentiation of gamma oscillatory activity through repetitive transcranial magnetic stimulation of the dorsolateral prefrontal cortex. *Neuropsychopharmacology : Official Publication of the American College of Neuropsychopharmacology*, *34*(11), 2359–67. doi:10.1038/npp.2009.79

Benabid, A.-L., Pollak, P., Hoffmann, D., Gervason, C., Hommel, M., Perret, J. E., … Gao, D. M. (1991). Long-term suppression of tremor by chronic stimulation of the ventral intermediate thalamic nucleus. *The Lancet*, *337*(8738), 403–406.

Benabid, A.-L., Wallace, B., Mitrofanis, J., Xia, C., Piallat, B., Fraix, V., … Berger, F. (2005). Therapeutic electrical stimulation of the central nervous system. *Comptes Rendus Biologies*, *328*(2), 177–186. doi:10.1016/j.crvi.2004.10.011

Benazzouz, A., Piallat, B., Pollak, P., & Benabid, A.-L. (1995). Responses of substantia nigra pars reticulata and globus pallidus complex to high frequency stimulation of the subthalamic nucleus in rats: electrophysiological data. *Neuroscience Letters*, *189*(2), 77–80.

Benchenane, K., Tiesinga, P. H., & Battaglia, F. P. (2011). Oscillations in the prefrontal cortex : a gateway to memory and attention. *Current Opinion in Neurobiology*, *21*(3), 475–485. doi:10.1016/j.conb.2011.01.004

Berton, O., McClung, C. a, Dileone, R. J., Krishnan, V., Renthal, W., Russo, S. J., … Nestler, E. J. (2006). Essential role of BDNF in the mesolimbic dopamine pathway in social defeat stress. *Science*, *311*(5762), 864–8. doi:10.1126/science.1120972

Bewernick, B. H., Hurlemann, R., Matusch, A., Kayser, S., Grubert, C., Hadrysiewicz, B., … Schlaepfer, T. E. (2010). Nucleus accumbens deep brain stimulation decreases ratings of depression and anxiety in treatment-resistant depression. *Biological Psychiatry*, *67*(2), 110–6. doi:10.1016/j.biopsych.2009.09.013

Bewernick, B. H., Kayser, S., Sturm, V., & Schlaepfer, T. E. (2012). Long-Term Effects of Nucleus Accumbens Deep Brain Stimulation in Treatment-Resistant Depression : Evidence for Sustained Efficacy. *Neuropsychopharmacology*, *37*(9), 1975–1985. doi:10.1038/npp.2012.44

Boggio, P. S., Rigonatti, S. P., Ribeiro, R. B., Myczkowski, M. L., Nitsche, M. a, Pascual-Leone, A., & Fregni, F. (2008). A randomized, double-blind clinical trial on the efficacy of cortical direct current stimulation for the treatment of major depression. *International Journal of Neuropsychopharmacology*, *11*(2), 249–54. doi:10.1017/S1461145707007833

Brothers, L., Ring, B., & Kling, A. (1990). Response of neurons in the macaque amygdala to complex social stimuli. *Behavioural Brain Research*, *41*(3), 199–213. doi:10.1016/0166-4328(90)90108-Q

Burt, T., Lisanby, S. H., & Sackeim, H. A. (2002). Neuropsychiatric applications of transcranial magnetic stimulation: a meta analysis. *The International Journal of Neuropsychopharmacology*, *5*(01), 73–103.

Butson, C. R., Cooper, S. E., Henderson, J. M., & McIntyre, C. C. (2007). Patient-specific analysis of the volume of tissue activated during deep brain stimulation. *NeuroImage*, *34*(2), 661–70. doi:10.1016/j.neuroimage.2006.09.034

Buzsaki, G. (2006). *Rhythms of the Brain*. Oxford University Press.

Canli, T., Zhao, Z., Brewer, J., Gabrieli, J. D. E., & Cahill, L. (2000). Event-related activation in the human amygdala associates with later memory for individual emotional response. *The Journal of Neuroscience*.

Carmichael, S. T., & Price, J. L. (1995). Limbic connections of the orbital and medial prefrontal cortex in macaque monkeys. *Journal of Comparative Neurology*, *363*(4), 615–641.

Carpenter, L. L., Wyche, M. C., Friehs, G. M., & O'Reardon, J. P. (2009). Electroconvulsive Therapy, Transcranial Magnetic Stimulation, and Vagus Nerve Stimulation for Depression. In *Neuromodulation* (pp. 665–673).

Chen, R., Samii, A., Canos, M., Wassermann, E. M., & Hallett, M. (1997). Effects of phenytoin on cortical excitability in humans. *Neurology*, *49*, 881–883.

Chepenik, L. G., Raffo, M., Hampson, M., Lacadie, C., Wang, F., Jones, M. M., … Blumberg, H. P. (2010). Functional connectivity between ventral prefrontal cortex and amygdala at low frequency in the resting state in bipolar disorder. *Psychiatry Research*, *182*(3), 207–10. doi:10.1016/j.pscychresns.2010.04.002

Coenen, V. a, Schlaepfer, T. E., Maedler, B., & Panksepp, J. (2010). Cross-species affective functions of the medial forebrain bundle-Implications for the treatment of affective pain and depression in humans. *Neuroscience and Biobehavioral Reviews*, *35*(9), 1971–81. doi:10.1016/j.neubiorev.2010.12.009

Cohen, L. G., Roth, B. J., Wassermann, E. M., Topka, H., Fuhr, P., Schultz, J., & Hallett, M. (1991). Magnetic stimulation of the human cerebral cortex, an indicator of reorganization in motor pathways in certain pathological conditions. *Journal of Clinical Neurophysiology*, *8*(1), 56–65.

Cohen, L. G., Ziemann, U., Chen, R., Classen, J., Hallett, M., Gerloff, C., & Butefisch, C. (1998). Studies of neuroplasticity with transcranial magnetic stimulation. *Journal of Clinical Neurophysiology : Official Publication of the American Electroencephalographic Society*, *15*(4), 305–24. Retrieved from http://www.ncbi.nlm.nih.gov/pubmed/9736465

Cotter, D., Mackay, D., Landau, S., Kerwin, R., & Everall, I. (2001). Reduced Glial Cell Density and Neuronal Size in the Anterior Cingulate Cortex in Major Depressive Disorder. *Archives of General Psychiatry*, *58*, 545–553.

Dale, A. M., Fischl, B., & Sereno, M. I. (1999). Cortical Surface-Based Analysis I. Segmentation and Surface Reconstruction Anders. *NeuroImage*, *194*, 179–194.

Demitrack, M. A. (2007). The use and clinical significance of transcranial magnetic stimulation in the treatment of major depression. *Psychopharm Review*, *42*(6), 43–49.

Downar, J., & Daskalakis, Z. J. (2013). New targets for rTMS in depression: a review of convergent evidence. *Brain Stimulation*, *6*(3), 231–40. doi:10.1016/j.brs.2012.08.006

Drevets, W. C. (2001). Neuroimaging and neuropathological studies of depression : implications for the cognitive-emotional features of mood disorders. *Current Opinion in Neurobiology*, *11*, 240–249.

Drevets, W. C., Videen, T. O., Price, J. L., Preskorn, S. H., Carmichael, S. T., & Raichle, M. E. (1992). A functional anatomical study of unipolar depression. *The Journal of Neuroscience : the Official Journal of the Society for Neuroscience*, *12*(9), 3628–41. Retrieved from http://www.ncbi.nlm.nih.gov/pubmed/1527602

Etkin, A., Egner, T., & Kalisch, R. (2011). Emotional processing in anterior cingulate and medial prefrontal cortex. *Trends in Cognitive Sciences*, *15*(2), 85–93. doi:10.1016/j.tics.2010.11.004

Fingelkurts, A. A., Fingelkurts, A. A., Kivisaari, R., Pekkonen, E., Ilmoniemi, R. J., & Ka, S. (2004). Enhancement of GABA-Related Signalling Is Associated With Increase of Functional Connectivity in Human Cortex. *Human Brain Mapping*, *22*, 27–39. doi:10.1002/hbm.20014

Fitzgerald, P. B., Hoy, K., McQueen, S., Herring, S., Segrave, R., Been, G., … Daskalakis, Z. J. (2008). Priming stimulation enhances the effectiveness of low-frequency right prefrontal cortex transcranial magnetic stimulation in major depression. *Journal of Clinical Psychopharmacology*, *28*(1), 52–58. Retrieved from http://www.ncbi.nlm.nih.gov/pubmed/18204341

Fitzgerald, P. B., Hoy, K., McQueen, S., Maller, J. J., Herring, S., Segrave, R., … Daskalakis, Z. J. (2009). A randomized trial of rTMS targeted with MRI based neuro-navigation in treatment-resistant depression. *Neuropsychopharmacology : Official Publication of the American College of Neuropsychopharmacology*, *34*(5), 1255–62. doi:10.1038/npp.2008.233

Fox, M. D., Buckner, R. L., White, M. P., Greicius, M. D., & Pascual-Leone, A. (2012). Efficacy of Transcranial Magnetic Stimulation Targets for Depression Is Related to Intrinsic Functional Connectivity with the Subgenual Cingulate. *Biological Psychiatry*. doi:10.1016/j.biopsych.2012.04.028

Fox, M. D., Halko, M., Eldaief, M., & Pascual-Leone, A. (2012). Measuring and manipulating brain connectivity with resting state functional connectivity magnetic resonance imaging (fcMRI) and transcranial magnetic stimulation (TMS). *NeuroImage*.

Fregni, F., Boggio, P. S., Nitsche, M. A., Marcolin, M. A., Rigonatti, S. P., & Pascual-Leone, A. (2006). Letters to the Editor: Treatment of major depression with transcranial direct current stimulation. *Bipolar Disorders*, *8*(2), 203–205. doi:10.1111/j.1399-5618.2006.00291.x

Fujita, A., Nakaaki, S., Segawa, K., Azuma, H., Sato, K., Arahata, K., … others. (2006). Memory, attention, and executive functions before and after sine and pulse wave electroconvulsive therapies for treatment-resistant major depression. *The Journal of ECT*, *22*(2), 107–112.

Gabbott, P. L. A., Warner, T. A., Jays, P. R. L., & Bacon, S. J. (2003). Areal and synaptic interconnectivity of prelimbic (area 32), infralimbic (area 25) and insular cortices in the rat. *Brain Research*, *993*(1), 59–71.

George, M. S., Lisanby, S. H., & Sackeim, H. A. (1999). Transcranial magnetic stimulation: applications in neuropsychiatry. *Archives of General Psychiatry*, *56*(4), 300–11. Retrieved from http://www.ncbi.nlm.nih.gov/pubmed/20439832

Ghashghaei, H. T., Hilgetag, C. C., & Barbas, H. (2007). Sequence of information processing for emotions based on the anatomic dialogue between prefrontal cortex and amygdala. *NeuroImage*, *34*(3), 905–23. doi:10.1016/j.neuroimage.2006.09.046

Gloor, P., Olivier, A., Quesney, L. F., Andermann, F., & Horowitz, S. (1982). The role of the limbic system in experiential phenomena of temporal lobe epilepsy. *Annals of Neurology*, *12*(2), 129–144.

Greenberg, B. D. (2009). Deep Brain Stimulation for Highly Refractory Depression. In *Neuromodulation* (pp. 689–709).

Greicius, M. D., Flores, B. H., Menon, V., Glover, G. H., Solvason, H. B., Kenna, H., … Schatzberg, A. F. (2007). Resting-state functional connectivity in major depression: abnormally increased contributions from subgenual cingulate cortex and thalamus. *Biological Psychiatry*, *62*(5), 429–37. doi:10.1016/j.biopsych.2006.09.020

Gross, J., Baillet, S., Barnes, G. R., Henson, R. N., Hillebrand, A., Jensen, O., … Schoffelen, J.-M. (2013). Good practice for conducting and reporting MEG research. *NeuroImage*, *65*, 349–63. doi:10.1016/j.neuroimage.2012.10.001

Gruzelier, J. (2009). A theory of alpha / theta neurofeedback , creative performance enhancement , long distance functional connectivity and psychological integration. *Cognitive Processing*, *10*, 101–109. doi:10.1007/s10339-008-0248-5

Gutman, D. A., Holtzheimer, P. E., Behrens, T. E. J., Johansen-Berg, H., & Mayberg, H. S. (2009). A tractography analysis of two deep brain stimulation white matter targets for depression. *Biological Psychiatry*, *65*(4), 276–282. doi:10.1016/j.biopsych.2008.09.021

Hamani, C., Amorim, B. O., Wheeler, A. L., Diwan, M., Driesslein, K., Covolan, L., … Nobrega, J. N. (2014). Deep brain stimulation in rats: Different targets induce similar antidepressant-like effects but influence different circuits. *Neurobiology of Disease*, *71*, 205–214. doi:10.1016/j.nbd.2014.08.007

Hamani, C., Diwan, M., Isabella, S., Lozano, A. M., & Nobrega, J. N. (2010). Effects of different stimulation parameters on the antidepressant-like response of medial prefrontal cortex deep brain stimulation in rats. *Journal of Psychiatric Research*, *44*(11), 683–7. doi:10.1016/j.jpsychires.2009.12.010

Hamani, C., Diwan, M., Macedo, C. E., Brandão, M. L., Shumake, J., Gonzalez-Lima, F., … Nobrega, J. N. (2010). Antidepressant-like effects of medial prefrontal cortex deep brain stimulation in rats. *Biological Psychiatry*, *67*(2), 117–24. doi:10.1016/j.biopsych.2009.08.025

Hamani, C., Mayberg, H. S., Snyder, B., Giacobbe, P., Kennedy, S. H., & Lozano, A. M. (2009). Deep brain stimulation of the subcallosal cingulate gyrus for depression: anatomical location of active contacts in clinical responders and a suggested guideline for targeting. *Journal of Neurosurgery*, *111*(6), 1209–15. doi:10.3171/2008.10.JNS08763

Hamani, C., Mayberg, H. S., Stone, S., Laxton, A., Haber, S. N., & Lozano, A. M. (2011). The subcallosal cingulate gyrus in the context of major depression. *Biological Psychiatry*, *69*(4), 301–8. doi:10.1016/j.biopsych.2010.09.034

Hamani, C., & Nóbrega, J. N. (2010). Deep brain stimulation in clinical trials and animal models of depression. *The European Journal of Neuroscience*, *32*(7), 1109–17. doi:10.1111/j.1460-9568.2010.07414.x

Hamani, C., & Temel, Y. (2012). Deep brain stimulation for psychiatric disease: contributions and validity of animal models. *Science Translational Medicine*, *4*(142), 142rv8. doi:10.1126/scitranslmed.3003722

Hamilton, M. (1960). A rating scale for Depression. *Journal of Neurology, Neurosurgery and Psychiatry*, *23*, 56–62.

Herbsman, T., Avery, D., Ramsey, D., Holtzheimer, P. E., Wadjik, C., Hardaway, F., … Nahas, Z. (2009). More lateral and anterior prefrontal coil location is associated with better repetitive transcranial magnetic stimulation antidepressant response. *Biological Psychiatry*, *66*(5), 509–15. doi:10.1016/j.biopsych.2009.04.034

Hillebrand, A., Barnes, G. R., Bosboom, J. L., Berendse, H. W., & Stam, C. J. (2012). Frequency-dependent functional connectivity within resting-state networks: an atlas-based MEG beamformer solution. *NeuroImage*, *59*(4), 3909–21. doi:10.1016/j.neuroimage.2011.11.005

Holdefer, R. N., Sadleir, R., & Russell, M. J. (2006). Predicted current densities in the brain during transcranial electrical stimulation. *Clinical Neurophysiology : Official Journal of the International Federation of Clinical Neurophysiology*, *117*(6), 1388–97. doi:10.1016/j.clinph.2006.02.020

Holtzheimer, P. E., Kelley, M. E., Gross, R. E., Filkowski, M. M., Garlow, S. J., Barrocas, A., … Mayberg, H. S. (2012). Subcallosal Cingulate Deep Brain Stimulation for Treatment-Resistant Unipolar and Bipolar Depression. *Archives of General Psychiatry*, 1–9. doi:10.1001/archgenpsychiatry.2011.1456

Holtzheimer, P. E., & Mayberg, H. S. (2011). Deep brain stimulation for psychiatric disorders. *Annual Review of Neuroscience*, *34*, 289–307. doi:10.1146/annurev-neuro-061010-113638

Hoover, W. B., & Vertes, R. P. (2007). Anatomical analysis of afferent projections to the medial prefrontal cortex in the rat. *Brain Structure and Function*, *212*, 149–179. doi:10.1007/s00429-007-0150-4

Iremonger, K. J., Anderson, T. R., Hu, B., & Kiss, Z. H. T. (2006). Cellular mechanisms preventing sustained activation of cortex during subcortical high-frequency stimulation. *Journal of Neurophysiology*, *96*(2), 613–621.

Johansen-Berg, H., Gutman, D. A., Behrens, T. E. J., Matthews, P. M., Rushworth, M. F., Katz, E., … Mayberg, H. S. (2008). Anatomical connectivity of the subgenual cingulate region targeted with deep brain stimulation for treatment-resistant depression. *Cerebral Cortex (New York, N.Y. : 1991)*, *18*(6), 1374–83. doi:10.1093/cercor/bhm167

Jones, D. L., & Mogenson, G. J. (1980). Nucleus accumbens to globus pallidus GABA projection: Electrophysiological and iontophoretic investigations. *Brain Research*, *188*(1), 93–105. doi:10.1016/0006-8993(80)90559-4

Kelley, A. E., & Stinus, L. (1984). The distribution of the projection from the parataenial nucleus of the thalamus to the nucleus accumbens in the rat: an autoradiographic study. *Experimental Brain Research*, *54*(3), 499–512.

Kessler, R. C., Berglund, P., Demler, O., Jin, R., Merikangas, K. R., & Walters, E. E. (2005). Lifetime Prevalence and Age-of-Onset Distributions of DSM-IV Disorders in the National Comorbidity Survey Replication. *Archives of General Psychiatry*, *62*(593-602).

Klöppel, S., Bäumer, T., Kroeger, J., Koch, M. a, Büchel, C., Münchau, A., & Siebner, H. R. (2008). The cortical motor threshold reflects microstructural properties of cerebral white matter. *NeuroImage*, *40*(4), 1782–91. doi:10.1016/j.neuroimage.2008.01.019

Koenigs, M., & Grafman, J. (2009). The functional neuroanatomy of depression: distinct roles for ventromedial and dorsolateral prefrontal cortex. *Behavioural Brain Research*, *201*(2), 239–43. doi:10.1016/j.bbr.2009.03.004

Kopell, B. H., Halverson, J., Butson, C. R., Dickinson, M., Bobholz, J., Harsch, H., … Dougherty, D. D. (2011). Epidural cortical stimulation of the left dorsolateral prefrontal cortex for refractory major depressive disorder. *Neurosurgery*, *69*(5), 1015–29. doi:10.1227/NEU.0b013e318229cfcd

Krishnan, V., & Nestler, E. J. (2008). The molecular neurobiology of depression. *Nature*, *455*(7215), 894–902. doi:10.1038/nature07455

Le Doux, J. (1996). *The Emotional Brain: The Mysterious Underpinnings of Emotional Life*. Simon and Schuster.

Lefaucheur, J.-P. (2008). Principles of therapeutic use of transcranial and epidural cortical stimulation. *Clinical Neurophysiology*, *119*(10), 2179–84. doi:10.1016/j.clinph.2008.07.007

Lefaucheur, J.-P., Antal, A., Ahdab, R., Ciampi de Andrade, D., Fregni, F., Khedr, E. M., … Paulus, W. (2008). The use of repetitive transcranial magnetic stimulation (rTMS) and transcranial direct current stimulation (tDCS) to relieve pain. *Brain Stimulation*, *1*(4), 337–344. doi:10.1016/j.brs.2008.07.003

Leuchter, A. F., Cook, I. a, Hunter, A. M., Cai, C., & Horvath, S. (2012). Resting-state quantitative electroencephalography reveals increased neurophysiologic connectivity in depression. *PloS One*, *7*(2), e32508. doi:10.1371/journal.pone.0032508

Li, L., Ma, N., Li, Z., Tan, L., Liu, J., Gong, G., … Xu, L. (2007). Prefrontal white matter abnormalities in young adult with major depressive disorder: a diffusion tensor imaging study. *Brain Research*, *1168*, 124–8. doi:10.1016/j.brainres.2007.06.094

Liebetanz, D., Nitsche, M. a, Tergau, F., & Paulus, W. (2002). Pharmacological approach to the mechanisms of transcranial DC-stimulation-induced after-effects of human motor cortex excitability. *Brain : A Journal of Neurology*, *125*(Pt 10), 2238–47. Retrieved from http://www.ncbi.nlm.nih.gov/pubmed/12244081

Lim, K. O., & Helpern, J. a. (2002). Neuropsychiatric applications of DTI - a review. *NMR in Biomedicine*, *15*(7-8), 587–93. doi:10.1002/nbm.789

Lisanby, S. H. (2007). Electroconvulsive therapy for depression. *The New England Journal of Medicine*, *357*(19), 1939–45. doi:10.1056/NEJMct075234

Lozano, A. M., Mayberg, H. S., Giacobbe, P., Hamani, C., Craddock, R. C., & Kennedy, S. H. (2008). Subcallosal cingulate gyrus deep brain stimulation for treatment-resistant depression. *Biological Psychiatry*, *64*(6), 461–7. doi:10.1016/j.biopsych.2008.05.034

Lu, Q., Wang, Y., Luo, G., Li, H., & Yao, Z. (2013). Dynamic connectivity laterality of the amygdala under negative stimulus in depression: a MEG study. *Neuroscience Letters*, *547*, 42–7. doi:10.1016/j.neulet.2013.05.002

Malone, D. a, Dougherty, D. D., Rezai, A. R., Carpenter, L. L., Friehs, G. M., Eskandar, E. N., … Greenberg, B. D. (2009). Deep brain stimulation of the ventral capsule/ventral striatum for treatment-resistant depression. *Biological Psychiatry*, *65*(4), 267–75. doi:10.1016/j.biopsych.2008.08.029

Manola, L., Holsheimer, J., Veltink, P. H., & Buitenweg, J. R. (2007). Anodal vs cathodal stimulation of motor cortex: a modeling study. *Clinical Neurophysiology*, *118*(2), 464–74. doi:10.1016/j.clinph.2006.09.012

Manola, L., Roelofsen, B. H., Holsheimer, J., Marani, E., & Geelen, J. (2005). Modelling motor cortex stimulation for chronic pain control: electrical potential field, activating functions and responses of simple nerve fibre models. *Medical & Biological Engineering & Computing*, *43*(3), 335–43. Retrieved from http://www.ncbi.nlm.nih.gov/pubmed/16035221

Mayberg, H. S. (1997). Limbic-Cortical Dysregulation : A Proposed Model of Depression. *Journal of Neuropsychiatry*, *9*(3), 471–481.

Mayberg, H. S. (2003). Modulating dysfunctional limbic-cortical circuits in depression : towards development of brain-based algorithms for diagnosis and. *British Medical Bulletin*, *65*, 193–207. doi:10.1093/bmb/ldg65.193

Mayberg, H. S. (2009). Targeted electrode-based modulation of neural circuits for depression. *The Journal of Clinical Investigation*, *119*(4), 717–25. doi:10.1172/JCI38454

Mayberg, H. S., Lozano, A. M., Voon, V., McNeely, H. E., Seminowicz, D., Hamani, C., … Kennedy, S. H. (2005). Deep brain stimulation for treatment-resistant depression. *Neuron*, *45*(5), 651–60. doi:10.1016/j.neuron.2005.02.014

McDonald, A. ., Mascagni, F., & Guo, L. (1996). Projections of the medial and lateral prefrontal cortices to the amygdala: A phaseolus vulgaris leucoagglutinin study in the rat. *Neuroscience*, *71*, 55–75.

McIntyre, C. C., & Grill, W. M. (1999). Excitation of central nervous system neurons by nonuniform electric fields. *Biophysical Journal*, *76*(2), 878–88. doi:10.1016/S0006-3495(99)77251-6

McIntyre, C. C., Grill, W. M., Sherman, D. L., & Thakor, N. V. (2004). Cellular effects of deep brain stimulation: model-based analysis of activation and inhibition. *Journal of Neurophysiology*, *91*(4), 1457–69. doi:10.1152/jn.00989.2003

Miller, B. L., & Cummings, J. L. (2007). *The human frontal lobes: Functions and disorders*. Guilford press.

Mogenson, G. J., Swanson, L. W., & Wu, M. (1983). Neural Projections from Nucleus Accumbens to Globus Pallidus, Substantia Innominata, and Lateral Preoptic-Lateral Hypothalamic Area: An Anatomical and electrophysiological investigation in the rat. *The Journal of Neuroscience*, *3*, 189–202.

Monkul, E. S., Hatch, J. P., Nicoletti, M. a, Spence, S., Brambilla, P., Lacerda, a L. T., … Soares, J. C. (2007). Fronto-limbic brain structures in suicidal and non-suicidal female patients with major depressive disorder. *Molecular Psychiatry*, *12*(4), 360–6. doi:10.1038/sj.mp.4001919

Morris, J. S., Ohman, A., & Dolan, R. J. (1998). Conscious and unconscious emotional learning in the human amygdala. *Nature*, *393*(June), 467–470.

Moscrip, T. D., Terrace, H. S., Sackeim, H. A., & Lisanby, S. H. (2006). Randomized controlled trial of the cognitive side-effects of magnetic seizure therapy (MST) and electroconvulsive shock (ECS). *The International Journal of Neuropsychopharmacology*, *9*(01), 1–11.

Muller, M. B., Toschi, N., Kresse, A. E., Post, A., & Keck, M. E. (2000). Long-Term Repetitive Transcranial Magnetic Stimulation Increases the Expression of Brain-Derived Neurotrophic Factor and Cholecystokinin mRNA , but not Neuropeptide Tyrosine mRNA in Specific Areas of Rat Brain. *Neuropsychopharmacology*, *23*, 205–215.

Nahas, Z. (2010). The frontiers in brain imaging and neuromodulation: a new challenge. *Frontiers in Psychiatry / Frontiers Research Foundation*, *1*(August), 25. doi:10.3389/fpsyt.2010.00025

Nahas, Z., Anderson, B. S., Borckardt, J., Arana, A. B., George, M. S., Reeves, S. T., & Takacs, I. (2010). Bilateral epidural prefrontal cortical stimulation for treatment-resistant depression. *Biological Psychiatry*, *67*(2), 101–9. doi:10.1016/j.biopsych.2009.08.021

Nahas, Z., Teneback, C. C., Kozel, F. A., Speer, A. M., DeBrux, C., Molloy, M., … George, M. S. (2001). Brain effects of TMS delivered over prefrontal cortex in

depressed adults: role of stimulation frequency and coil-cortex distance. *The Journal of Neuropsychiatry and Clinical Neurosciences*, *13*(4), 459–470. Retrieved from http://www.ncbi.nlm.nih.gov/pubmed/11748315

Nakamura, H., Kitagawa, H., Kawaguchi, Y., & Tsuji, H. (1997). Intracortical facilitation and inhibition after transcranial magnetic stimulation in conscious humans. *Journal of Physiology*, 817–823.

Nauta, W. J. H., & Domesick, V. B. (1984). Afferent and efferent relationships of the basal ganglia. In *Ciba Foundation Symposium 107-Functions of the Basal Ganglia* (pp. 3–29).

Nestler, E. J., & Carlezon, W. a. (2006). The mesolimbic dopamine reward circuit in depression. *Biological Psychiatry*, *59*(12), 1151–9. doi:10.1016/j.biopsych.2005.09.018

Nestor, K. a, Jones, J. D., Butson, C. R., Morishita, T., Jacobson, C. E., Peace, D. a, … Okun, M. S. (2014). Coordinate-based lead location does not predict Parkinson's disease deep brain stimulation outcome. *PloS One*, *9*(4), e93524. doi:10.1371/journal.pone.0093524

Nunez, P. L., & Silberstein, R. B. (2000). On the relationship of synaptic activity to macroscopic measurements: does co-registration of EEG with fMRI make sense? *Brain Topography*, *13*(2), 79–96. Retrieved from http://www.ncbi.nlm.nih.gov/pubmed/11154104

O'Reardon, J. P., Solvason, H. B., Janicak, P. G., Sampson, S. M., Isenberg, K. E., Nahas, Z., … Sackeim, H. a. (2007). Efficacy and safety of transcranial magnetic stimulation in the acute treatment of major depression: a multisite randomized controlled trial. *Biological Psychiatry*, *62*(11), 1208–16. doi:10.1016/j.biopsych.2007.01.018

Ongur, D., Drevets, W. C., & Price, J. L. (1998). Glial reduction in the subgenual prefrontal cortex in. *Proceedings of the National Academy of Sciences*, *95*(October), 13290–13295.

Papanicolaou, A. C. (2009). *Clinical Magnetoencephalography and Magnetic Source Imaging*. Cambridge University Press.

Pascual-Leone, A., Tarazona, F., Keenan, J., Tormos, J. M., Hamilton, R., & Catala, M. D. (1999). Transcranial magnetic stimulation and neuroplasticity. *Neuropsychologia*, *37*(2), 207–217. Retrieved from http://www.ncbi.nlm.nih.gov/pubmed/10080378

Pathak, Y., Kopell, B. H., Szabo, A., Rainey, C., Harsch, H., & Butson, C. R. (2012). The role of electrode location and stimulation polarity in patient response to cortical

stimulation for major depressive disorder. *Brain Stimulation*, 1–7. doi:10.1016/j.brs.2012.07.001

Petsche, H. (1996). Approaches to verbal , visual and musical creativity by EEG coherence analysis. *International Journal of Psychophysiology*, *24*, 145–159.

Petty, F. (1995). GABA and mood disorders : a brief review and hypothesis. *Journal of Affective Disorders*, *34*, 275–281.

Phelps, E. A., Labar, K. S., & Spencer, D. D. (1997). Memory for Emotional Words Following Unilateral Temporal Lobectomy. *Brain and Cognition*, *109*(35), 85–109.

Pittenger, C., & Duman, R. S. (2008). Stress , Depression , and Neuroplasticity : A Convergence of Mechanisms. *Neuropsychopharmacology Reviews*, 88–109. doi:10.1038/sj.npp.1301574

Quirk, G. J., & Beer, J. S. (2006). Prefrontal involvement in the regulation of emotion: convergence of rat and human studies. *Current Opinion in Neurobiology*, *16*(6), 723–7. doi:10.1016/j.conb.2006.07.004

Rajkowska, G., Wei, J., Dilley, G., Pittman, S. D., Meltzer, H. Y., Overholser, J. C., … Stockmeier, C. A. (1999). Morphometric Evidence for Neuronal and Glial Prefrontal Cell Pathology in Major Depression *. *Society of Biological Psychiatry*, *3223*(99), 1085–1098.

Ramasubbu, R., & MacQueen, G. (2010). Using Neuroimaging to Predict Outcome in Patients with Major Depressive Disorder. *Mind & Brain, The Journal of Psychiatry*, *1*(2), 59–68. doi:10.1080/10401230500464661

Ranck, J. B. (1975). Which elements are excited in electrical stimulation of mammalian central nervous system: A review. *Brain Research*, *98*(3), 417–440. doi:10.1016/0006-8993(75)90364-9

Rauch, S. L., Dougherty, D. D., Malone, D. A., Rezai, A. R., Friehs, G. M., Fischman, A. J., … Greenberg, B. D. (2006). A functional neuroimaging investigation of deep brain stimulation in patients with obsessive–compulsive disorder. *Journal of Neurosurgery*, *104*, 558–565.

Ressler, K. J., & Mayberg, H. S. (2007). Targeting abnormal neural circuits in mood and anxiety disorders: from the laboratory to the clinic. *Nature Neuroscience*, *10*(9), 1116–24. doi:10.1038/nn1944

Ridding, M. C., & Rothwell, J. C. (2007). Is there a future for therapeutic use of transcranial magnetic stimulation?, *8*(July), 559–567.

Riva-Posse, P., Sueng Choi, K., Holtzheimer, P. E., McIntyre, C. C., Gross, R. E., Chaturvedi, A., … Mayberg, H. S. (2014). Defining Critical White Matter Pathways Mediating Successful Subcallosal Cingulate Deep Brain Stimulation for Treatment-Resistant Depression. *Biological Psychiatry*, 1–7. doi:10.1016/j.biopsych.2014.03.029

Roth, B. J., Saypol, J. M., Hallett, M., & Cohen, L. G. (1991). A theoretical calculation of the electric field induced in the cortex during magnetic stimulation. *Electroencephalography and Clinical Neurophysiology/Evoked Potentials Section*, *81*(1), 47–56. doi:10.1016/0168-5597(91)90103-5

Rush, A. J., Trivedi, M. H., Wisniewski, S. R., Nierenberg, A. A., Stewart, J. W., Warden, D., … Fava, M. (2006). Acute and longer-term outcomes in depressed outpatients requiring one or several treatment steps: a STAR*D report. *Am J Psychiatry*, *163*(11), 1905–17. doi:10.1176/appi.ajp.163.11.1905

Sackeim, H. A. (2001). Functional brain circuits in major depression and remission. *Archives of General Psychiatry*, *58*(7), 649–650. Retrieved from http://www.ncbi.nlm.nih.gov/pubmed/11448370

Sakkalis, V. (2011). Review of advanced techniques for the estimation of brain connectivity measured with EEG/MEG. *Computers in Biology and Medicine*, *41*(12), 1110–7. doi:10.1016/j.compbiomed.2011.06.020

Schlaepfer, T. E., Bewernick, B. H., Kayser, S., Mädler, B., & Coenen, V. a. (2013). Rapid effects of deep brain stimulation for treatment-resistant major depression. *Biological Psychiatry*, *73*(12), 1204–12. doi:10.1016/j.biopsych.2013.01.034

Schlaepfer, T. E., Cohen, M. X., Frick, C., Kosel, M., Brodesser, D., Axmacher, N., … Sturm, V. (2008). Deep Brain Stimulation to Reward Circuitry Alleviates Anhedonia in Refractory Major Depression. *Neuropsychopharmacology*, *33*, 368–377. doi:10.1038/sj.npp.1301408

Schoffelen, J.-M., & Gross, J. (2009). Source connectivity analysis with MEG and EEG. *Human Brain Mapping*, *30*(6), 1857–65. doi:10.1002/hbm.20745

Shimizu, E., Hashimoto, K., Okamura, N., Koike, K., Komatsu, N., Kumakiri, C., … Iyo, M. (2003). Alterations of serum levels of brain-derived neurotrophic factor (BDNF) in depressed patients with or without antidepressants. *Biological Psychiatry*, *54*(1), 70–75. doi:10.1016/S0006-3223(03)00181-1

Siebner, H. R., Bergmann, T. O., Bestmann, S., Massimini, M., Johansen-Berg, H., Mochizuki, H., … Rossini, P. M. (2009). Consensus paper: combining transcranial stimulation with neuroimaging. *Brain Stimulation*, *2*(2), 58–80. doi:10.1016/j.brs.2008.11.002

Tadel, F., Baillet, S., Mosher, J. C., Pantazis, D., & Leahy, R. M. (2011). Brainstorm: a user-friendly application for MEG/EEG analysis. *Computational Intelligence and Neuroscience, 2011*, 879716. doi:10.1155/2011/879716

Takagishi, M., & Chiba, T. (1991). Efferent projections of the infralimbic (area 25) region of the medial prefrontal cortex in the rat: an anterograde tracer PHA-L study. *Brain Research*, *566*(1), 26–39.

Taulu, S., Simola, J., & Kajola, M. (2005). Applications of the Signal Space Separation Method. *IEEE Transactions on Signal Processing*, *53*(9), 3359–3372.

Thielscher, A., Opitz, A., & Windhoff, M. (2011). Impact of the gyral geometry on the electric field induced by transcranial magnetic stimulation. *NeuroImage*, *54*(1), 234–43. doi:10.1016/j.neuroimage.2010.07.061

Thut, G., & Pascual-Leone, A. (2010). Integrating TMS with EEG : How and What For? *Brain Topography, 22*, 215–218. doi:10.1007/s10548-009-0128-z

Usuda, I., Tanaka, K., & Chiba, T. (1998). Efferent projections of the nucleus accumbens in the rat with special reference to subdivision of the nucleus : biotinylated dextran amine study. *Brain Research, 797*, 73–93.

Veerakumar, A., Challis, C., Gupta, P., Da, J., Upadhyay, A., Beck, S. G., & Berton, O. (2013). Antidepressant-like effects of cortical deep brain stimulation coincide with pro-neuroplastic adaptations of serotonin systems. *Biological Psychiatry*.

Veith, R. C., Lewis, N., Linares, O. A., Barnes, R. F., Raskind, M. A., Villacres, E., … Halter, J. B. (1994). Sympathetic Nervous system Activity in Major Depression. *Archives of General Psychiatry*, *51*, 411–422.

Vertes, R. P. (2004). Differential projections of the infralimbic and prelimbic cortex in the rat. *Synapse, 51*(1), 32–58. doi:10.1002/syn.10279

Walsh, V., & Cowey, A. (2000). Transcranial magnetic stimulation and cognitive neuroscience. *Nature Reviews Neuroscience, 1*(1), 73–79. doi:10.1038/35036239

Warden, M. R., Selimbeyoglu, A., Mirzabekov, J. J., Lo, M., Thompson, K. R., Kim, S.-Y., … Deisseroth, K. (2012). A prefrontal cortex-brainstem neuronal projection that controls response to behavioural challenge. *Nature*, *492*(7429), 428–432.

Wongsarnpigoon, A., & Grill, W. M. (2008). Computational modeling of epidural cortical stimulation. *Journal of Neural Engineering*, *5*(4), 443–54. doi:10.1088/1741-2560/5/4/009

Yue, L., Xiao-lin, H., & Tao, S. (2009). The effects of chronic repetitive transcranial magnetic stimulation on glutamate and gamma-aminobutyric acid in rat brain. *Brain Research, 1260,* 94–9. doi:10.1016/j.brainres.2009.01.009